



Loma Linda University Electronic Theses, Dissertations & Projects

9-2018

Estimating Root Volumes by Limited Segmentation: A Volumetric Analysis of CBCT and Micro-CT Data

Theresa C. Baldwin

Follow this and additional works at: <https://scholarsrepository.llu.edu/etd>



Part of the [Orthodontics and Orthodontology Commons](#)

Recommended Citation

Baldwin, Theresa C., "Estimating Root Volumes by Limited Segmentation: A Volumetric Analysis of CBCT and Micro-CT Data" (2018). *Loma Linda University Electronic Theses, Dissertations & Projects*. 504.
<https://scholarsrepository.llu.edu/etd/504>

This Thesis is brought to you for free and open access by TheScholarsRepository@LLU: Digital Archive of Research, Scholarship & Creative Works. It has been accepted for inclusion in Loma Linda University Electronic Theses, Dissertations & Projects by an authorized administrator of TheScholarsRepository@LLU: Digital Archive of Research, Scholarship & Creative Works. For more information, please contact scholarsrepository@llu.edu.

LOMA LINDA UNIVERSITY
School of Dentistry
in conjunction with the
Faculty of Graduate Studies

Estimating Root Volumes by Limited Segmentation: A Volumetric Analysis of CBCT
and Micro-CT Data

by

Theresa C. Baldwin

A Thesis submitted in partial satisfaction of
the requirements for the degree
Master of Science in Orthodontics and Dentofacial Orthopedics

September 2018

© 2018

Theresa C. Baldwin
All Rights Reserved

Each person whose signature appears below certifies that this thesis in his/her opinion is adequate, in scope and quality, as a thesis for the degree Master of Science.

_____, Chairperson
Joseph M. Caruso, Professor, Orthodontics and Dentofacial Orthopedics

Gregory Olson, Associate Professor, Orthodontics and Dentofacial Orthopedics

Kitichai Rungcharassaeng, Professor, Orthodontics and Dentofacial Orthopedics

ACKNOWLEDGEMENTS

I would like to thank the members of my committee, Dr. Joseph Caruso, Dr. Kitichai Rungcharassaeng, and Dr. Gregory Olson, for their guidance and advice throughout this process. I would also like to thank Dr. Gina Roque-Torres for providing her knowledge and time, Seth Myhre for his technical assistance, and Udochukwu Oyoyo for lending his statistical expertise. Additionally, I would like to thank the assistants at the Loma Linda University Orthodontic Clinic, specifically Marianne, Jose, Victor, and Shannon who provided invaluable guidance with training and operation of the NewTom™ 5G CBCT scanner.

To my family and friends, without your love and support this dream would not have come to fruition. You kept me going when all hope was lost, and for that I will be forever grateful. And finally, I would like to thank God for providing me with the strength and opportunity to achieve this amazing accomplishment.

CONTENTS

| | |
|--|------|
| Approval Page..... | iii |
| Acknowledgements..... | iv |
| List of Figures | vii |
| List of Tables | viii |
| List of Abbreviations | ix |
| Abstract..... | x |
| Chapter | |
| 1. Review of the Literature | 1 |
| Cone Beam Computed Tomography | 1 |
| Radiation Exposure..... | 2 |
| Data Acquisition and Reconstruction | 3 |
| Segmentation and Volumetric Analysis..... | 7 |
| Micro-CT | 8 |
| Orthodontic Applications and Future Considerations..... | 9 |
| 2. Estimating Root Volumes by Limited Segmentation: A Volumetric Analysis of CBCT and Micro-CT Data | 10 |
| Abstract..... | 11 |
| Introduction..... | 13 |
| Null Hypothesis | 14 |
| Materials and Methods..... | 15 |
| Tooth Selection | 15 |
| CBCT Image Acquisition and Reconstruction | 15 |
| Micro-CT Image Acquisition and Reconstruction..... | 17 |
| Segmentation..... | 17 |
| CBCT | 17 |
| Micro-CT | 18 |
| Axial Slice Reduction | 18 |
| CBCT | 18 |

| | |
|---|----|
| Volumetric Reconstruction | 19 |
| CBCT | 19 |
| Micro-CT | 21 |
| Data Collection | 21 |
| Statistical Analysis..... | 23 |
| Results..... | 23 |
| Volume..... | 24 |
| Voxel Count | 29 |
| Length | 29 |
| Grayscale Values | 30 |
| Discussion..... | 31 |
| Volume..... | 31 |
| Voxel Count..... | 32 |
| Length | 33 |
| Grayscale Values | 33 |
| Effect of Interpolation Approach | 34 |
| Reliability..... | 35 |
| Limitations of the Study and Recommendations for Future Studies | 35 |
| Conclusions..... | 36 |
| References..... | 38 |
| 3. Discussion..... | 42 |
| Extended Discussion..... | 42 |
| Future Studies | 42 |
| Appendices | |
| A. Raw Data..... | 44 |

FIGURES

| Figures | Page |
|--|------|
| 1. Images of Five Extracted Teeth | 16 |
| 2. Coronal, Sagittal, and Axial Views – Maxillary Left First Premolar | 20 |
| 3. Superimpositions of 100% Mask and 3D Wrap – Maxillary Left First Premolar | 22 |

TABLES

| Tables | Page |
|---|------|
| 1. Reliability Test and ICC Table | 23 |
| 2. Means Table - Volume..... | 25 |
| 3. Means Table – Voxel Count | 26 |
| 4. Means Table – Length | 27 |
| 5. Means Table – Grayscale Values..... | 28 |

ABBREVIATIONS

| | |
|-------|--|
| 2D | Two-Dimensional |
| 3D | Three-Dimensional |
| ALARA | As Low As Reasonably Achievable |
| BMP | Bitmap file format |
| CBCT | Cone Beam Computed Tomography |
| CEJ | Cementoenamel Junction |
| CT | Computed Tomography |
| DICOM | Digital Imaging and Communications in Medicine |
| FOV | Field of View |
| FSV | First Scout View |
| ICC | Intraclass Correlation Coefficient |
| IRB | Institutional Review Board |
| MTF | Modulation Transfer Function |
| SSV | Second Scout View |
| TAD | Temporary Anchorage Device |
| TMD | Temporomandibular Disorder |
| TMJ | Temporomandibular Joint |

ABSTRACT OF THE THESIS

Estimating Root Volumes by Limited Segmentation: A Volumetric Analysis of CBCT and Micro-CT Data

by

Theresa C. Baldwin

Master of Science, Graduate Program in Orthodontics and Dentofacial Orthopedics
Loma Linda University, September 2018
Dr. Joseph M. Caruso, Chairperson

Introduction: The increased dimensional accuracy of images provided by cone beam computed tomography (CBCT) scans allows for more in-depth diagnosis and treatment planning. Expedient interpolation of segmented data that provides clinically acceptable results will encourage clinicians to frequently use CBCT images for clinical/radiographic evaluation. Some of these applications include, quantification of root resorption, determination of force required for specific tooth movements, and customized appliances.

Purpose: The study had two purposes. The first was to compare the accuracy of digital tooth volumes acquired from CBCT to the gold standard, micro-computed tomography (micro-CT). The second was to determine the effect of axial slice reduction on volume interpolation, using two different interpolation methods.

Materials & Methods: Five unrestored, single-rooted teeth underwent micro-CT and CBCT scanning. The data was reconstructed and imported into Simpleware™ ScanIP for segmentation and volumetric analysis. Segmentation was completed, resulting in a mask, which then underwent sequential root reduction. Two interpolation methods, Three Dimensional (3D) Wrap and Interpolation Toolbox, were applied to each reduction mask. The volume, length, voxel count, and grayscale values of each method were evaluated.

Statistical analysis was performed using intraclass correlation coefficient (ICC) tests to examine intraexaminer reliability, Friedman's Analysis of Variance by Ranks to evaluate the mean difference between micro-CT and CBCT, Wilcoxon Signed Rank Test to evaluate the reduction differences between two CBCT resolutions, and Kruskal-Wallis test to evaluate the differences in reduction within each CBCT resolution. The significance level of all statistical analysis was set at $\alpha = 0.05$.

Results: The volume comparisons between micro-CT and CBCT scans showed statistically significant differences ($p = 0.015$), however, pairwise comparison revealed the difference to be between the two resolutions of CBCT scans and not between CBCT and micro-CT. With regard to sequential reductions and interpolation accuracy, the 3D Wrap method had a greater tendency toward underestimation while the Interpolation Toolbox method provided more accurate measurements.

Conclusions: Due to small sample size and statistically significant differences between overall mean volume measurements, it cannot be concluded that micro-CT and CBCT scans produce the same volume. Interpolated digital tooth volume obtained from axial reductions was more accurate with the Interpolation Toolbox method, than the 3D Wrap method. It can be concluded that the Interpolation Toolbox method would be beneficial for tooth volume assessment in a clinical setting.

CHAPTER ONE

REVIEW OF THE LITERATURE

Cone Beam Computed Tomography

Orthodontic diagnosis and treatment planning utilizes various imaging methods to ensure satisfactory progress and outcomes. For decades, traditional two-dimensional (2D) radiographs, lateral cephalometric tracings, and photographs have been the standard.²⁸ In the 1980s, cone beam computed tomography (CBCT), originally introduced for use in angiography, was implemented in oral and maxillofacial imaging. In the late 1990s, the cost of CBCT technology decreased, as well as its footprint, allowing it to be introduced into the dental office.²⁸ Following suit, in 2001, the Food and Drug Administration approved the first CBCT scanner, identified as the NewTom™ QR-DVT 9000.¹ The QR-DVT 9000 was the first commercial CBCT system dedicated to dento-maxillo-facial imaging.²⁶ Imaging quality and diagnostic accuracy of the NewTom™ QR-DVT 9000 was analyzed in a study by Mozzo et al., which concluded that continued manufacture of low-cost CBCT machines for use in dentistry was allowable to satisfy the growing demand for such an imaging modality.²⁶ Likewise, CBCT has gained popularity in orthodontic practice due to its ability to provide reliable, high resolution images at reduced cost with increased precision.²⁷ Furthermore, CBCT images are anatomically true to size, as opposed to conventional cephalometric radiographs.^{7,8,23} As an added benefit, CBCT prevents unnecessary expense, scan time, and increased radiation, more common in traditional computed tomography (CT) units.^{2,5,6}

Common orthodontic applications for CBCT include, but are not limited to, temporomandibular joint (TMJ) evaluation, assessment of skeletal jaw relationships,

examination of impacted teeth, airway visualization, orthognathic surgery treatment planning, preparation for placement of temporary anchorage devices (TAD), assessment of root resorption, and growth estimation.^{5,27}

Radiation Exposure

As orthodontic offices have begun substituting CBCT scans for more traditional imaging methods, risk of increased patient radiation exposure comes to the forefront. Therefore, a balanced approach is necessary to prioritize patient health alongside the need for diagnostic accuracy.^{3,29} The American Dental Association Council on Scientific Affairs recommends the principle of “As low as reasonably achievable,” (ALARA) to guide professionals when determining the necessity for dental radiography.¹ ALARA provides that radiographs should be taken based upon patient need, with the image(s) fulfilling the clinician’s purpose (i.e. accurate diagnosis and treatment planning).¹

Since 1990, allowable exposure to radiation risk has been identified as the “effective dose.”³⁰ For example, the effective radiation dose of CBCT ranges from 20 μSv to 599 μSv , depending upon the machine used.³¹ Traditional imaging methods, such as a full-mouth series with rectangular collimation, panoramic radiographs, and lateral cephalometric radiographs, have effective radiation doses of 35 μSv , 9-26 μSv , and 3-6 μSv , respectively.³¹ In response to the increased use of CBCT imaging in orthodontic practice, imaging machines with adjustable settings that offer one low (2 mA) and one high (15 mA) dose are recommended. Thus allowing clinicians to select a radiation dose that will provide a more accurate diagnostic assessment, if necessary.¹ However, despite the benefits of CBCT in orthodontic diagnosis and treatment planning, increased patient

radiation exposure prevents its routine use.²⁷

Data Acquisition and Reconstruction

CBCT data can be viewed in two dimensions with axial, sagittal, and coronal views as well as in three dimensions by way of volumetric reconstruction.²⁵ Unlike 2D techniques, CBCT rapidly generates multiple single projection images, commonly known as basis projection images (projection data). This imaging sequence prevents structure overlap, allowing for more precise visualization.^{28,32} The 2D basis projection images being captured are then converted to 3D through algorithmic manipulation in a process called primary reconstruction.^{28,33} Secondary reconstruction allows the clinician to reformat the images for more traditional radiographic examination (lateral cephalogram, panoramic image, posterior anterior cephalogram) as well as for better visualization of specific structures (cross-sectional reconstruction).³⁴

Specifically, QR Verona, the manufacturer of all NewTom™ CBCT machines, introduced SmartBeam™ technology with the initial machine, the NNT 9000. The frontal and lateral scout films, used for positioning of the patient for proper imaging, also are used to determine the density of the patient. The machine then automatically adjusts the exposure to provide the lowest effective dose to the patient by continuous monitoring and delivering intermittent bursts of radiation, rather than a continuous dose.³⁵

Traditionally, relevant settings include, milliamperes (mA), peak kilovoltage (kVp), scan time, field of view (FOV), voxel size, and spatial resolution.^{5,11,29}

Milliamperes refer to the tube *current*, while peak kilovoltage refers to the tube *voltage*. These two parameters are the primary determinants of radiation exposure.²⁸

More advanced CBCT systems provide the option of adjustable scan time. Longer scan time results in higher contrast and spatial resolution. Conversely, shorter scan times produce a lower resolution image but reduce the amount of radiation and the risk of patient movement. Thus, shorter scan times are often satisfactory for most orthodontic needs.³⁶

Field of view (FOV) refers to the size of the scan volume necessary to adequately capture the region of interest. FOV varies depending upon the size of the object being imaged, and is produced by the shape and size of the detector, collimation, and beam projection geometry. CBCT systems differ by available proprietary FOV options. These are often represented by pre-programmed settings of increased FOV including but not limited to, localized region, single arch, interarch, maxillofacial, and craniofacial. Logically, the larger the FOV, the more structures included in the image.^{28,37,38} Adjusting the FOV, however, affects both spatial resolution and voxel size, thus a smaller FOV results in increased spatial resolution and smaller voxel size.¹⁸

Spatial resolution refers to the ability of an imaging system to delineate fine details of an object. Quality of spatial resolution depends upon the detector system used and is affected by sensor pixel size, gray-level resolution, and reconstruction technique.³⁹ Common detector systems include flat-panel and image intensifier. Flat-panel detectors render volumes that are cylindrical-shaped, whereas image intensifier detectors produce spherical-shaped volumes. Both detectors are similar in sensitivity, however, the contrast and dynamic range is greater with flat-panel detectors.³⁶ As a result, most current CBCT machines use a flat-panel detector, allowing for heightened resolution of the original projection images.

Accuracy in measuring spatial resolution is most successful through modulation transfer function (MTF). MTF uses a computer algorithm to analyze contrast and provide and accurate measurement of spatial resolution. Detector image acquisition involves a multi-step process, including initial capture, refinement, and noise reduction. Consequently, this can lead to sampling artifacts and an increase in MTF. As a result, the enhanced spatial resolution can be falsely depicted.³⁹

The spatial resolution of an image is determined by the density of 3D pixels, otherwise known as voxels. Voxels are individual volume elements that make up a 3D image. Detector resolution in 3D imaging systems determines voxel size, which can range from 0.09 mm to 0.4 mm for CBCT systems, with even smaller sizes employed in micro-CT imaging. CBCT units generally have isotropic voxels (each voxel has the same dimension in all three planes of space) allowing for the same resolution of data in axial and coronal slices.^{28,29,37,38,40} Similar to spatial resolution, CBCT voxel size is determined by the focal spot size of the x-ray tube, the x-ray geometric configuration, and the pixel size of the solid state detector.²⁸

Each voxel has its own associated grayscale value based upon the amount of radiation absorbed. If a single voxel contains tissue types of varying densities, the grayscale within that voxel is averaged during 3D reconstruction.^{14,28} The grayscale values in CBCT images cannot be used quantitatively due to voxel averaging. This differs from conventional CT imaging, where the exact densities are known and corresponding grayscale values have been determined and defined as Hounsfield units.^{14,22} It should be noted that the grayscale bit depth of the CBCT system has an effect on image quality. Although the human eye can see approximately the equivalent of a 10-bit grayscale

(1,024 shades of gray), most current CBCT machines range from 12- to 16-bit grayscale (4,096 – 65,536 shades of gray). Reconstruction software is able to use the higher grayscale values during primary and secondary reconstruction, resulting in increased detail within the volume. Ultimately, these higher grayscale values are discernable by the user due to the software's ability to manipulate the gray values.³⁶

The dimensional accuracy of a CBCT scan can also be influenced by threshold settings, smoothing filters, proximity of surrounding tissue, and artifacts present in the image.⁹ The software included with each CBCT system also has an impact on the quality of the reconstruction. The output data is limited by the applicable algorithm's ability to remove noise, artifacts, and to properly distinguish between densities. These variables also tend to shift among different versions of the same software.³⁶

Artifacts can cause significant distortion of an image, which may lead to inaccurate volumetric calculations.⁶ The most commonly encountered artifacts include: beam hardening artifacts, partial volume effect, ring artifacts, motion artifacts, and artifacts caused by noise and scatter. Beam hardening artifacts appear as dark streaks and are caused by metal present within the object being imaged. The metal absorbs the lower wavelength x-rays, resulting in less x-rays being recorded on the detector than were emitted inducing an error into the recorded data.^{41,42} Partial volume effects, seen in all CT images, result from the averaging that occurs with imaging of tissues of different densities. Such effects show as blurred junctions between tissue types or image degradation resulting in loss of structures.²⁸ Ring artifacts occur with defective or uncalibrated detector elements which manifest as concentric rings around the axis of rotation, generally the axial plane in CBCT imaging. Motion artifacts appear with

misalignment of source, object, or detector. A double image is the most common motion artifact and can be reduced with sufficient fixation of the patient's head.⁴¹ Noise and scatter can also cause image-depreciating artifacts. Noise within a scan produces inconsistent grayscale values while scatter yields streaks within a volume, similar to beam hardening artifacts.^{41,42}

Segmentation & Volumetric Analysis

Recent introduction of CBCT imaging into the field of orthodontics has popularized the concept of volumetric analysis for both anatomic visualization and biomechanical considerations.¹⁰ Volumetric analysis requires segmentation of an object, such as a tooth, from its surrounding structures.^{2,11} Segmentation essentially refers to removal of all surrounding structures for better visualization of the area of interest, and in turn, relies upon semi-automated or manual image thresholding. Thresholding is the process of breaking an image into many smaller images whose boundaries are defined by grayscale values. Common thresholding methods are identified as “global,” “local,” and “adaptive.” Global thresholding can be applied when components of the image and the background are consistent throughout the entire volume. If there is uneven illumination, local thresholding can be used to partition the image before global thresholding. Adaptive thresholding is narrowly used when uneven *background* illumination exists and foreground image separation is necessary.¹³ Once a thresholding interval has been defined, voxels containing gray values within this interval are then used to reconstruct the 3D segmented image.^{12,13}

Image segmentation can be a challenging process, subject to human bias.³³ The

challenges of CBCT tooth segmentation arise from proximity and density of surrounding bone, variations in tooth density, proximity of adjacent teeth, and existing restorations.¹⁴ Due to the general limitations in CBCT contrast resolution and lack of segmentation standardization, most methods still involve manual segmentation.^{2,11} This necessitates individual slice segmentation, which is time consuming and undesirable in a clinical setting.¹² Thus, semi-automated segmentation, with manual intervention for refinement, is preferred.^{10,15} A study by Forst et al., concluded that semi-automatic segmentation, with manual refinement, generated the most reliable measurements as opposed to automatic-only and manual-only segmentation methods.¹⁵

Completion of segmentation results in an image that represents the area of interest, known as a mask. This mask can then be duplicated and manipulated as needed. In many instances, smoothing filters are applied. These are software-specific algorithms that take partial volume effects into account in an attempt to generate a more accurate image surface.⁴² In reality, smoothing functions have been shown to reduce the structural accuracy by 3%-12%.¹⁵ Additional inaccuracies can also result from variances in scanning software algorithms, scan resolution, bone thickness, and user proficiency.⁶

Micro-CT

Micro-CT is regarded as the reference standard in dental 3D imaging for the volumetric analysis of hard tissues, due to its ability to produce high resolution images (up to three micrometers, 0.018 mm voxel), with only one scan.²⁻⁴ However, the evaluation of materials by micro-CT is only possible *ex vivo* (outside of the body), with scan time being several hours. Consequently, micro-CT is more accurately suited for a

research setting. Therefore, for the purpose of this study, micro-CT provides an accurate comparison.^{2,44}

Orthodontic Applications & Future Considerations

The advantages of CBCT have been discussed in previous literature and include but are not limited to, reconstructed lateral cephalograms, accurate superimpositions due to a 1:1 measuring ratio, ability to reorient of the patient's head to counteract improper positioning, create separate right and left images for more precise assessment of asymmetries and superior analysis of impacted and transposed teeth, airway, TMJ, TAD placement, and cleft lip and palate conditions.^{8,9} Additional software developments allow facial photos to be combined with CBCT images for examination of the relationship between hard and soft tissues. This has the potential to assist in surgical planning, and tooth movement for extraction and/or multidisciplinary cases. Lastly, the ability to superimpose two 3D volumes can provide the clinician with increased information on treatment outcomes and stability.^{9,16} Because of the scalable use of the CBCT volume, it is important that we continue to develop clinically applicable utilities that can maximize the information yield.

CHAPTER TWO
ESTIMATING ROOT VOLUMES BY LIMITED SEGMENTATION: A
VOLUMETRIC ANALYSIS OF CBCT AND MICRO-CT DATA

By

Theresa Baldwin, D.D.S., M.A.

Master of Science, Graduate Program in Orthodontics and Dentofacial Orthopedics

Loma Linda University, September 2018

Dr. Joseph Caruso, Chairperson

Abstract

Introduction: The increased dimensional accuracy of images provided by cone beam computed tomography (CBCT) scans allows for more in-depth diagnosis and treatment planning. Expedient interpolation of data that provides clinically acceptable results will encourage clinicians to frequently use CBCT images for clinical/radiographic evaluation. Some of these applications include, quantification of root resorption, determination of force required for specific tooth movements, and customized appliances.

Purpose: The study had two purposes. The first was to compare the accuracy of digital tooth volumes acquired from CBCT to the gold standard, micro-computed tomography (micro-CT). The second was to determine the effect of axial slice reduction on volume interpolation, using two different interpolation methods.

Materials & Methods: Five unrestored, single-rooted teeth underwent micro-CT and CBCT scanning. The data was reconstructed and imported into Simpleware™ ScanIP for segmentation and volumetric analysis. Segmentation was completed, resulting in a mask, which then underwent sequential root reduction. Two interpolation methods, Three Dimensional (3D) Wrap and Interpolation Toolbox, were applied to each reduction mask. The volume, length, voxel count, and grayscale values of each method were evaluated. Statistical analysis was performed using intraclass correlation coefficient (ICC) tests to examine intraexaminer reliability, Friedman's Analysis of Variance by Ranks to evaluate the mean difference between micro-CT and CBCT, Wilcoxon Signed Rank Test to evaluate the reduction differences between two CBCT resolutions, and Kruskal-Wallis test to evaluate the differences in reduction within each CBCT resolution. The significance level of all statistical analysis was set at $\alpha = 0.05$.

Results: The volume comparisons between micro-CT and CBCT scans showed statistically significant differences ($p = 0.015$), however, pairwise comparison revealed the difference to be between the two resolutions of CBCT scans and not between CBCT and micro-CT. With regard to sequential reductions and interpolation accuracy, the 3D Wrap method had a greater tendency toward underestimation while the Interpolation Toolbox method provided more accurate measurements.

Conclusions: Due to small sample size and statistically significant differences between overall mean volume measurements, it cannot be concluded that micro-CT and CBCT scans produce the same volume. Interpolated digital tooth volume obtained from axial reductions was more accurate with the Interpolation Toolbox method, than the 3D Wrap method. It can be concluded that the Interpolation Toolbox method would be beneficial for tooth volume assessment in a clinical setting.

Introduction

With the advent of CBCT for use in oral and maxillofacial imaging in 2001, the field of orthodontics gained the opportunity for increased diagnostic ability, with relative ease of implementation into everyday orthodontic practice.¹ Micro-CT is considered as the reference standard in 3D dental imaging for the quantification of hard tissues due to the production of exceptionally high resolution images.²⁻⁴ However, one significant advantage of CBCT over micro-CT is its ability to assess structures *in vivo*.⁴

CBCT images are true to size, offering diagnostic quality without the expense, scan time, and increased radiation, common with traditional computed tomography (CT) units.^{2,5-8} The ability to generate reconstructed lateral cephalograms provides for digital reorientation of the head for more precise assessment of asymmetries, increased accuracy of superimpositions, and to counteract patient positioning errors.^{8,9} Additionally, CBCT affords clinicians the opportunity to pinpoint the exact location of impacted and transposed teeth to aid in determination of the most efficient route of movement into the arch, accurate measurement of interproximal bone and distance between roots for ease of temporary anchorage device (TAD) placement, and temporomandibular joint (TMJ) visualization and evaluation in patients with temporomandibular disorders (TMD).⁹

The introduction of CBCT imaging to the field of orthodontics has popularized the idea of volumetric analysis for both anatomic visualization and biomechanical considerations.¹⁰ Volumetric analysis necessitates segmentation of the tooth from its surrounding structures.^{2,11} In turn, segmentation involves determination of a thresholding value based upon desired gray values within the object being segmented.^{12,13} Concerning oral structures, specifically teeth, global thresholding is often the method of choice for

precise segmentation.¹³ Challenges associated with segmentation of teeth include, proximity of surrounding bone and adjacent teeth, varying densities within each tooth, and presence of existing restorations.¹⁴ Although time consuming, semi-automatic segmentation with manual intervention for refinement has been shown to be the most reliable method of segmentation.¹⁵ Upon completion of segmentation, software programs are available for data manipulation. Despite many advances in CBCT technology, the need for clinically acceptable, easily implemented, methods for data manipulation remains. To date, no simple method exists to obtain measurements (volume, length, surface area) of a CBCT scanned tooth without first segmenting the entire structure, and then applying algorithms for the desired assessment. Additionally, no studies specifically examine the relationship between interpolation methods and structural consistency.

The purpose of the current study was to compare the gold standard (micro-CT) to CBCT scans of varying voxel size and field of view (FOV), to evaluate the accuracy of digital tooth volume. Furthermore, the effect of interpolation methods on root structure axial slice reduction will also be evaluated for accuracy in volume measurements.

Null Hypothesis

1. The first null hypothesis states that the digital tooth volume acquired from CBCT is no different than the digital tooth volume acquired from micro-CT.
2. The second null hypothesis states that the interpolated tooth volume calculated from segmented axial slices is the same regardless of the number of slices employed.

Materials and Methods

Tooth Selection

This study was deemed exempt from the Institutional Review Board (IRB) of Loma Linda University (LLU), Loma Linda, CA (IRB # 5170475). Five extracted permanent teeth were obtained from a previously IRB approved study at LLU. These teeth represented all four quadrants of the mouth and included, maxillary right lateral incisor, maxillary left canine, maxillary left second premolar, mandibular left first premolar, and mandibular right central incisor (Figure 1). The inclusion criteria required all teeth to be intact, unrestored, single-rooted, and disease free. No patient identifiers were apparent on the teeth. Before scanning, each tooth was cleaned with a hand scaler to remove as much residual bone and tissue as possible without excess removal of tooth structure.

CBCT Image Acquisition and Reconstruction

Each tooth was individually inserted, root first, into a 3" x 4" x 3" block of FloraCraft[®] Wet Foam and soaked for 30 minutes to ensure complete water absorption. The block was then positioned in the gantry in supine position with the apex directed cranially and the crown directed caudally. Each foam block was individually scanned using the NewTom[™] 5G CBCT unit (QR s.r.l., Verona, Italy). Two different scanning protocols were used for each tooth, one small FOV with high-resolution (CBCT₁₂), and one large FOV with low resolution (CBCT₁₈). The high-resolution, CBCT₁₂, scan parameters included, 12x8 FOV with 0.125 mm slice thickness, and 26 second scan time.

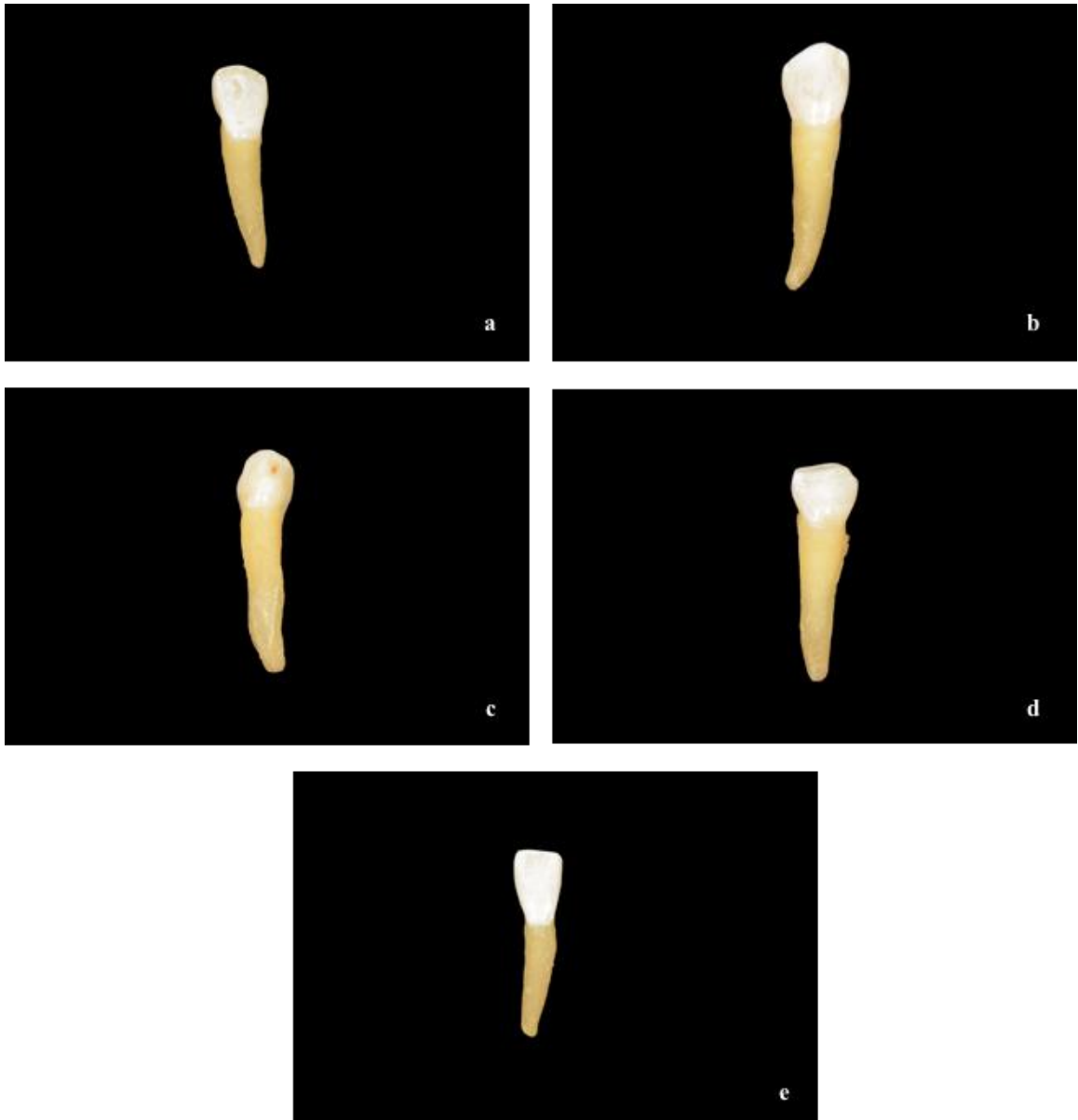


Figure 1. Five teeth used in study. (a) Maxillary right lateral incisor, (b) maxillary left canine, (c) maxillary left second premolar, (d) mandibular left first premolar, (e) mandibular right central incisor.

The low-resolution, CBCT₁₈, scan parameters included, 18x16 FOV, 0.3 mm slice thickness, and 26 second scan time. In total, 10 scans were acquired. After acquisition, the images were reconstructed using NNT™ software (Version 5.1; QR s.r.l., Verona, Italy) and exported in digital imaging and communications in medicine (DICOM) format.

Micro-CT Image Acquisition & Reconstruction

Each tooth was individually placed inside a plastic tube filled with water, and then positioned within the Skyscan™ 1272 micro-CT unit (Bruker, Belgium). The tooth was scanned at 80 kV, 125 μ A, at an isotropic pixel size of 26.5 μ m, performed by 180° rotation around the vertical axis. A camera exposure time of 2400 ms, rotation step of 0.8°, and frame averaging of 3 was used. X-rays were filtered with a 1mm aluminum filter. A flat-field correction was taken on the day prior to scanning to correct for variation in the pixel sensitivity of the camera. After acquisition, images were reconstructed using NRecon™ reconstruction software (Version 1.6.3; Bruker, Belgium) with a beam hardening coefficient of 20%, smoothing of 2, and an attenuation coefficient range of 0.06. This provided 672 axial cross-sections of the inner structure of each sample. The images were exported in bitmap (BMP) file format.

Segmentation

CBCT

Each tooth was individually imported as a DICOM file into Simpleware™ ScanIP (Version 2018.03; Synopsys, Inc., Mountain View, USA). The threshold was determined by manual adjustment of the upper and lower grayscale values and applied to all slices,

resulting in a mask. The unpaint tool was then used on individual active slices of the mask to remove any residual bone or noise within each scan. This resulted in a mask representing 100% of the tooth structure. No smoothing functions were applied to prevent inconsistencies due to possible shrinkage or enlargement.

Micro-CT

Each individual tooth was imported into Simpleware™ ScanIP in BMP file format with a defined spacing value of 0.0265 mm. The threshold was determined in the same manner used above for the CBCT scanned teeth, and a segmented mask was produced.

Axial Slice Reduction

CBCT

Once segmented, and determination of the 100% mask was complete, the CBCT scanned teeth then underwent a series of reduction of the root volume via deletion of axial slices of the mask until only the cementoenamel junction (CEJ) [including crown], midroot, and apex remained. The crown (incisal edge/occlusal tip to CEJ) was not reduced due to inconsistencies in interpolation resulting from variations in crown morphology and software algorithms.

First, the incisal edge/occlusal tip and apex were determined by choosing the smallest axial slice with at least 5 voxels (corresponding to a paint brush size of 3) to allow for increased interpolation accuracy. Due to software constraints, axial slices with less than 5 voxels do not allow for proper interpolation. Based upon visible grayscale

values, the CEJ was then determined to be at the last axial slice with distinguishable enamel on any surface (buccal, lingual, mesial, or distal) [Figure 2]. The midroot axial slice was determined by subtracting the CEJ axial slice from the apex and dividing by two. This number was then added to the CEJ slice to give the midroot axial slice number. Each subsequent 50% root reduction was made by duplicating the previous reduction mask and using the unpaint tool. One-by-one the unpaint tool was used on each active slice to reduce the root structure. The “CEJ, Midroot, Apex” mask was reduced using the “selection” option with unpaint, allowing for reduction of multiple slices at once, rather than one-by-one. Reductions resulting in less than two axial slices between CEJ and apex were not analyzed due to inaccurate interpolation. Due to variations in tooth length, only two teeth were reduced to 3.125% remaining root structure. This data was not included in statistical analysis due to a sample size of only two.

Volumetric Reconstruction

CBCT

After all reduction masks were completed, with the exception of the 100% mask, each mask was duplicated twice and missing slices were added using two different approaches, the “Interpolation toolbox” and the “3D Wrap.” These functions are located within the “Image processing” tab within Simpleware™ ScanIP.

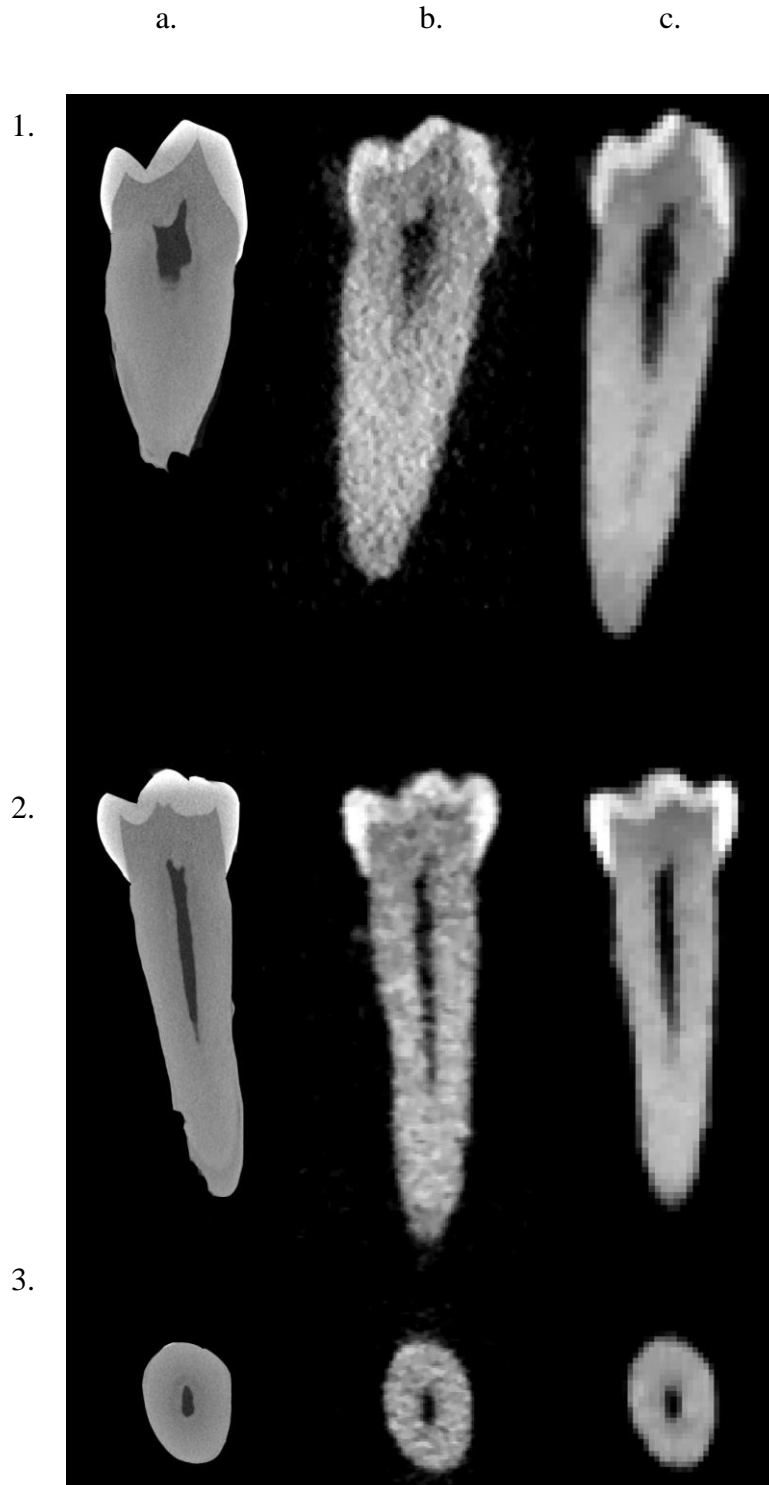


Figure 2. (1) Sagittal, (2) coronal, and (3) axial views of mandibular left first premolar. (a) Micro-CT, (b) CBCT₁₂, (c) CBCT₁₈. Increased noise is visible in the CBCT₁₂ scan.

The 100% mask was duplicated once and the 3D Wrap function was applied to evaluate the smoothing effects of this approach. The Interpolation toolbox approach is not applicable without slice reductions, as its purpose is to fill in missing slices without any smoothing effects. Figure 3 shows the effect of the 3D Wrap approach on tooth structure and volume.

Micro-CT

The micro-CT scans did not undergo sequential reduction of the root structure and therefore did not require interpolation of the root structure. The 100% mask was duplicated and the 3D Wrap function was applied in the same manor used above for the CBCT 100% mask.

Data Collection

Simpleware™ ScanIP has the intrinsic ability to provide quantitative data related to each mask. Upon completion of segmentation, root reduction, and volumetric reconstruction of each tooth, the “mask statistics” component was selected to evaluate four parameters of each mask, volume, length, voxel count, and grayscale values. The statistics templates chosen to provide this data were “General Statistics” and “Orientation of all masks.” This data was then exported as a CSV file format and compiled into one Microsoft™ Excel spreadsheet and saved in XLSX file format.



Figure 3. This figure shows a comparison of the 100% mask and the 3D Wrap approach for the mandibular left first premolar, and each scan group. The white represents the 100% mask. The red represents the 100% mask with the 3D Wrap applied. (a) Micro-CT, (b) CBCT₁₂, (c) CBCT₁₈.

Statistical Analysis

All statistical tests were nonparametric with 95% confidence intervals ($\alpha=0.05$), and unadjusted significance values. All tests were performed using SPSS™ software (Version 25.0; SPSS, Inc., Chicago, IL, USA). Friedman's Two-way Analysis of Variance by Ranks Test was used to examine the differences between the gold standard, micro-CT, and CBCT₁₂ and CBCT₁₈. To compare the sequential root reductions between CBCT₁₂ and CBCT₁₈, the Wilcoxon Signed Rank Test was used. To examine the sequential root reductions within CBCT₁₂ and CBCT₁₈, the reductions were subjected to independent samples Kruskal-Wallis Test.

One examiner performed all segmentations and axial slice reductions. This was repeated three times for each tooth over a period of one month. A reliability test was run and stratified for each scan modality using intraclass correlation coefficient (ICC) test and Cronbach's alpha.

Results

The intraexaminer reliability of segmentation and axial slice reduction was very high, with ICC values of 1.000, 0.999, and 0.995 for micro-CT, CBCT₁₂, and CBCT₁₈ respectively (Table 1).

Table 1. Reliability Test, ICC values for micro-CT, CBCT₁₂, and CBCT₁₈.

| | Cronbach's Alpha | Intraclass Coefficient | p-value |
|--------------------|------------------|------------------------|---------|
| Micro-CT | 1.000 | 1.000 | < 0.001 |
| CBCT ₁₂ | 1.000 | 0.999 | < 0.001 |
| CBCT ₁₈ | 0.998 | 0.995 | < 0.001 |

Volume

Table 2 shows the mean volume and standard deviation for micro-CT, CBCT₁₂, and CBCT₁₈. The mean volume comparison of CBCT₁₂ and CBCT₁₈ to micro-CT showed an overall statistically significant difference for both approaches among the three groups. Pairwise comparison for the reduction approach indicated the significance was between CBCT₁₂ and CBCT₁₈ ($p = 0.004$), while the 3D Wrap approach showed the significance between CBCT₁₈ and micro-CT ($p = 0.004$).

The comparison of approaches between CBCT₁₂ and CBCT₁₈ revealed CBCT₁₈ to have slightly larger mean volumes than CBCT₁₂ for the Reduction and Interpolation Toolbox approaches. The 3D Wrap approach, however, had mean CBCT₁₈ volumes that were smaller than CBCT₁₂. The Reduction approach showed a statistically significant difference in volume for the 50%, 25% and CEJ masks. The 3D Wrap and Interpolation Toolbox approaches, however showed a statistically significant difference for all masks except the CEJ mask.

The mean volume within the three approaches for CBCT₁₂ reduction masks were compared to the 100% original mask. For each of the approaches, the reduction masks were statistically similar to the 100% original mask. The mean volume for the reduction approach, unlike the 3D Wrap and Interpolation Toolbox approaches, showed a clinically significant decreasing trend with each subsequent reduction, however the null cannot be rejected. Likewise, the mean volume within the three approaches for CBCT₁₈ reduction masks were compared to the 100% original mask. For each approach, the reduction masks were statistically similar to the 100% original mask. The results were similar to those obtained for CBCT₁₂.

Table 2. Comparison of mean volumes using $\alpha=0.05$, $n=5$.

| Volume (mm ³) | | | | |
|---------------------------|----------------------------------|----------------------------------|---------------------------------|---------|
| Mean \pm SD | | | | |
| Reduction | Micro-CT | CBCT ₁₂ | CBCT ₁₈ | p-value |
| 100% OR | 446.0 \pm 165.5 ^{a,b} | 444.8 \pm 169.5 ^a | 467.2 \pm 168.7 ^b | 0.015 |
| 50% | - | 324.8 \pm 118.8 ^a | 343.6 \pm 118.0 ^b | 0.042 |
| 25% | - | 264.8 \pm 93.9 ^a | 282.4 \pm 93.9 ^b | 0.043 |
| 12.5% | - | 235.0 \pm 81.2 | 251.2 \pm 81.3 | 0.078 |
| 6.25% | - | 220.0 \pm 75.5 | 236.2 \pm 75.7 | 0.078 |
| CEJ | - | 208.8 \pm 70.1 ^a | 229.8 \pm 72.2 ^b | 0.043 |
| p-value | - | 0.136 | 0.084 | - |
| 3D Wrap | Micro-CT | CBCT ₁₂ | CBCT ₁₈ | p-value |
| 100% OR | 446.0 \pm 165.5 ^{a,b} | 444.8 \pm 169.5 ^a | 467.2 \pm 168.7 ^b | 0.015 |
| 100% | 473.8 \pm 177.3 ^a | 461.6 \pm 183.0 ^{a,b} | 343.4 \pm 146.8 ^b | 0.015 |
| 50% | - | 440.8 \pm 172.1 ^a | 363.8 \pm 150.9 ^b | 0.043 |
| 25% | - | 439.0 \pm 172.0 ^a | 361.8 \pm 153.0 ^b | 0.043 |
| 12.50% | - | 439.6 \pm 171.8 ^a | 359.4 \pm 157.1 ^b | 0.043 |
| 6.25% | - | 440.2 \pm 172.1 ^a | 351.0 \pm 156.4 ^b | 0.043 |
| CEJ | - | 410.6 \pm 157.3 ^a | 315.8 \pm 148.1 ^b | 0.043 |
| p-value | - | 0.982 | 0.895 | - |
| Interpolation | Micro-CT | CBCT ₁₂ | CBCT ₁₈ | p-value |
| Toolbox | - | - | - | - |
| 100% OR | - | 444.8 \pm 169.5 ^a | 467.20 \pm 168.7 ^b | 0.043 |
| 50% | - | 445.2 \pm 169.9 ^a | 467.20 \pm 168.7 ^b | 0.043 |
| 25% | - | 445.0 \pm 169.8 ^a | 468.00 \pm 169.0 ^b | 0.043 |
| 12.5% | - | 444.4 \pm 169.5 ^a | 467.00 \pm 168.9 ^b | 0.043 |
| 6.25% | - | 443.6 \pm 170.1 ^a | 465.20 \pm 169.5 ^b | 0.042 |
| CEJ | - | 411.6 \pm 156.1 ^a | 446.00 \pm 160.5 ^b | 0.043 |
| p-value | - | 0.963 | 0.967 | - |

^{a,b}Different letter denotes statistical significance between groups.

Table 3. Comparison of mean voxel counts using $\alpha=0.05$, $n=5$.

| Voxel Count (10^4) | | | | |
|------------------------|-----------------------------------|-------------------------------|------------------------------|---------|
| Mean \pm SD | | | | |
| Reduction | Micro-CT | CBCT ₁₂ | CBCT ₁₈ | p-value |
| 100% OR | 2400.00 \pm 890.00 ^a | 22.80 \pm 8.69 ^b | 1.73 \pm 0.62 ^c | 0.007 |
| 50% | - | 16.60 \pm 6.09 ^a | 1.27 \pm 0.44 ^b | 0.043 |
| 25% | - | 13.60 \pm 4.81 ^a | 1.05 \pm 0.35 ^b | 0.043 |
| 12.5% | - | 12.00 \pm 4.17 ^a | 0.93 \pm 0.30 ^b | 0.043 |
| 6.25% | - | 11.30 \pm 3.86 ^a | 0.88 \pm 0.28 ^b | 0.043 |
| CEJ | - | 10.70 \pm 3.60 ^a | 0.85 \pm 0.27 ^b | 0.043 |
| p-value | - | 0.130 | 0.084 | - |
| 3D Wrap | | | | |
| Reduction | Micro-CT | CBCT ₁₂ | CBCT ₁₈ | p-value |
| 100% OR | 2400.00 \pm 890.00 ^a | 22.80 \pm 8.69 ^b | 1.73 \pm 0.62 ^c | 0.007 |
| 100% | 2550.00 \pm 954.00 ^a | 23.60 \pm 9.38 ^b | 1.27 \pm 0.54 ^c | 0.007 |
| 50% | - | 22.60 \pm 8.80 ^a | 1.35 \pm 0.56 ^b | 0.043 |
| 25% | - | 22.50 \pm 8.81 ^a | 1.34 \pm 0.57 ^b | 0.043 |
| 12.50% | - | 22.50 \pm 8.79 ^a | 1.33 \pm 0.58 ^b | 0.043 |
| 6.25% | - | 22.50 \pm 8.82 ^a | 1.30 \pm 0.58 ^b | 0.043 |
| CEJ | - | 21.00 \pm 8.05 ^a | 1.17 \pm 0.55 ^b | 0.043 |
| p-value | - | 0.983 | 0.895 | - |
| Interpolation | | | | |
| Toolbox | Micro-CT | CBCT ₁₂ | CBCT ₁₈ | p-value |
| 100% OR | - | 22.80 \pm 8.69 ^a | 1.73 \pm 0.62 ^b | 0.043 |
| 50% | - | 22.80 \pm 8.69 ^a | 1.73 \pm 0.63 ^b | 0.043 |
| 25% | - | 22.80 \pm 8.70 ^a | 1.73 \pm 0.63 ^b | 0.043 |
| 12.5% | - | 22.80 \pm 8.68 ^a | 1.73 \pm 0.63 ^b | 0.043 |
| 6.25% | - | 22.70 \pm 8.69 ^a | 1.72 \pm 0.63 ^b | 0.043 |
| CEJ | - | 21.10 \pm 8.00 ^a | 1.65 \pm 0.60 ^b | 0.043 |
| p-value | - | 0.955 | 0.969 | - |

^{a,b,c} Different letter denotes statistical significance between groups.

Table 4. Comparison of mean length using $\alpha=0.05$, $n=5$.

| Length (mm) | | | | |
|---------------|----------------|--------------------|--------------------|---------|
| Mean \pm SD | | | | |
| Reduction | Micro-CT | CBCT ₁₂ | CBCT ₁₈ | p-value |
| 100% OR | 24.6 \pm 2.9 | 24.3 \pm 2.9 | 24.3 \pm 2.8 | 0.211 |
| 50% | - | 24.3 \pm 2.9 | 24.3 \pm 2.8 | 1.000 |
| 25% | - | 24.3 \pm 2.9 | 24.3 \pm 2.8 | 1.000 |
| 12.5% | - | 24.3 \pm 2.9 | 24.3 \pm 2.8 | 1.000 |
| 6.25% | - | 24.3 \pm 3.0 | 24.3 \pm 2.9 | 0.705 |
| CEJ | - | 23.0 \pm 4.0 | 24.3 \pm 2.8 | 0.109 |
| p-value | - | 0.952 | 1.000 | - |
| 3D Wrap | Micro-CT | CBCT ₁₂ | CBCT ₁₈ | p-value |
| 100% OR | 24.6 \pm 2.9 | 24.3 \pm 2.9 | 24.3 \pm 2.8 | 0.211 |
| 100% | 24.1 \pm 3.5 | 23.8 \pm 2.9 | 21.7 \pm 2.7 | 0.015 |
| 50% | - | 24.0 \pm 2.8 | 22.6 \pm 2.9 | 0.042 |
| 25% | - | 23.9 \pm 3.0 | 22.6 \pm 3.0 | 0.042 |
| 12.50% | - | 23.9 \pm 2.9 | 22.6 \pm 2.9 | 0.041 |
| 6.25% | - | 23.9 \pm 2.9 | 22.6 \pm 2.9 | 0.042 |
| CEJ | - | 23.8 \pm 2.9 | 21.5 \pm 3.3 | 0.043 |
| p-value | - | 0.987 | 0.690 | - |
| Interpolation | Micro-CT | CBCT ₁₂ | CBCT ₁₈ | p-value |
| 100% OR | - | 24.3 \pm 2.9 | 24.3 \pm 2.8 | 0.496 |
| 50% | - | 24.5 \pm 2.9 | 24.3 \pm 2.8 | 0.496 |
| 25% | - | 24.3 \pm 2.9 | 24.3 \pm 2.8 | 1.000 |
| 12.5% | - | 24.3 \pm 2.9 | 24.3 \pm 2.8 | 1.000 |
| 6.25% | - | 24.3 \pm 2.9 | 24.3 \pm 2.8 | 1.000 |
| CEJ | - | 24.3 \pm 2.9 | 24.3 \pm 2.8 | 1.000 |
| p-value | - | 0.996 | 1.000 | - |

Table 5. Comparison of mean grayscale count using $\alpha=0.05$, $n=5$.

| Grayscale Count | | | | |
|-----------------|------------------------------|---------------------------------|---------------------------------|---------|
| Mean \pm SD | | | | |
| Reduction | Micro-CT | CBCT ₁₂ | CBCT ₁₈ | p-value |
| 100% OR | 156.0 \pm 5.5 ^b | 2470.0 \pm 328.4 ^a | 2156.0 \pm 419.1 ^b | 0.015 |
| 50% | - | 2512.0 \pm 376.1 | 2208.0 \pm 467.4 | 0.080 |
| 25% | - | 2550.0 \pm 416.4 | 2254.0 \pm 512.1 | 0.136 |
| 12.5% | - | 2572.0 \pm 448.7 | 2286.0 \pm 542.4 | 0.138 |
| 6.25% | - | 2588.0 \pm 467.6 | 2300.0 \pm 561.9 | 0.176 |
| CEJ | - | 2604.0 \pm 486.6 | 2312.0 \pm 574.3 | 0.225 |
| p-value | - | 0.551 | 0.717 | - |
| 3D Wrap | Micro-CT | CBCT ₁₂ | CBCT ₁₈ | p-value |
| 100% OR | 156.0 \pm 5.5 ^b | 2470.0 \pm 328.4 ^a | 2156.0 \pm 419.1 ^b | 0.015 |
| 100% | 149.6 \pm 5.9 ^b | 2320.0 \pm 154.6 ^a | 2160.0 \pm 357.4 ^b | 0.015 |
| 50% | - | 2430.0 \pm 328.2 | 2200.0 \pm 421.8 | 0.138 |
| 25% | - | 2432.0 \pm 322.4 | 2200.0 \pm 422.9 | 0.138 |
| 12.50% | - | 2428.0 \pm 323.8 | 2194.0 \pm 418.7 | 0.138 |
| 6.25% | - | 2422.0 \pm 315.8 | 2178.0 \pm 411.1 | 0.138 |
| CEJ | - | 2404.0 \pm 264.8 | 2158.0 \pm 396.2 | 0.138 |
| p-value | - | 0.757 | 0.997 | - |
| Interpolation | Micro-CT | CBCT ₁₂ | CBCT ₁₈ | p-value |
| 100% OR | - | 2470.0 \pm 328.4 | 2156.0 \pm 419.1 | 0.080 |
| 50% | - | 2470.0 \pm 328.4 | 2156.0 \pm 419.1 | 0.080 |
| 25% | - | 2468.0 \pm 330.0 | 2154.0 \pm 416.0 | 0.080 |
| 12.5% | - | 2468.0 \pm 329.3 | 2152.0 \pm 413.7 | 0.078 |
| 6.25% | - | 2464.0 \pm 331.5 | 2146.0 \pm 399.1 | 0.080 |
| CEJ | - | 2474.0 \pm 304.0 | 2154.0 \pm 395.0 | 0.078 |
| p-value | - | 0.888 | 0.990 | - |

^{a,b}Different letter denotes statistical significance between groups.

Voxel Count

Table 3 shows the mean voxel count and standard deviation for micro-CT, CBCT₁₂ and CBCT₁₈. The difference in overall voxel count was statistically significant between micro-CT and CBCT both the Reduction and 3D Wrap approaches. Pairwise comparison for both approaches indicated the significance was between micro-CT and CBCT₁₈ ($p = 0.002$).

The comparison of approaches between CBCT₁₂ and CBCT₁₈ showed statistically significant differences, with the exception of the CEJ reduction. Overall, the mean voxel counts were less for CBCT₁₈ than CBCT₁₂.

The mean voxel count within the three approaches for CBCT₁₂ reduction masks were compared to the 100% original mask. For each of the parameters and approaches, the reduction masks were statistically similar to the 100% original mask. When voxel counts were examined, the means for the Reduction approach decreased with each subsequent reduction. The 3D Wrap and Interpolation Toolbox approaches remained consistent with only minor fluctuations noted among the subsequent reductions. Similarly, when the mean voxel count within the three approaches for CBCT₁₈ reduction masks were compared to the 100% original mask, the reduction masks were statistically similar to the 100% original mask.

Length

Table 4 shows the mean length and standard deviation for micro-CT, CBCT₁₂ and CBCT₁₈. Comparison of mean length between CBCT and micro-CT for the Reduction approach showed no statistical significance, indicating minimal variation in length

between the two groups. The 3D Wrap approach, however, did show statistical significance between groups. Pairwise comparison indicated the significance was between CBCT₁₈ and micro-CT ($p = 0.004$).

When CBCT₁₂ and CBCT₁₈ were compared, similar results were reported. The length means for Reduction and Interpolation Toolbox approaches showed no significant differences. The 3D Wrap, however, had significantly different means between CBCT₁₂ and CBCT₁₈ for all reductions.

The mean length within the three approaches for CBCT₁₂ and CBCT₁₈ reduction masks were compared to the 100% original mask. The means for length remained consistent for all three approaches within each group.

Grayscale Values

Table 5 shows the mean grayscale and standard deviation for micro-CT, CBCT₁₂ and CBCT₁₈. Mean grayscale values for both the Reduction and 3D Wrap approaches were significantly different between micro-CT and CBCT. Pairwise comparison indicated the significance was between micro-CT and CBCT₁₂ for both approaches ($p = 0.004$). The mean grayscale values decreased with increasing voxel size.

The mean CBCT₁₈ grayscale values were smaller than the CBCT₁₂ values. However, for each of the three approaches, the difference in grayscale values between groups was not significant.

The mean grayscale values within the three approaches for CBCT₁₂ and CBCT₁₈ reduction masks were compared to the 100% original mask. For each of the parameters and approaches, the reduction masks were statistically similar to the 100% original mask.

The mean grayscale values for the Reduction approach increased with each subsequent reduction while the 3D Wrap and Interpolation Toolbox approaches remained consistent with slight fluctuations noted among the subsequent reductions.

Discussion

With the increased use of CBCT in orthodontic practice, the applications of 3D imaging are sure to evolve with advances in CBCT technology and expanding software capability. Currently, CBCT data can be used to generate 3D printed models, provide dimensionally accurate lateral cephalograms, visualize growth, aid in age estimation, and evaluate oral and maxillofacial structures that cannot be accurately assessed with traditional 2D radiographs.^{16,17}

To ensure proper implementation and usage of CBCT data, the accuracy and reliability of measurements must be substantiated. The current study sought to examine the effects of resolution on four measures (volume, voxel count, grayscale values, and length). To achieve this objective, micro-CT was used as the gold standard to which two resolutions of CBCT were compared (CBCT₁₂, 125 μm and CBCT₁₈, 300 μm). Additionally, two different interpolation algorithms were tested to see if data removed by sequential root reduction could be accurately replaced.

Volume

The current study demonstrated a significant difference in mean volume measurements between micro-CT and CBCT₁₂ and CBCT₁₈. However, pairwise comparison revealed the significance to be between CBCT₁₂ and CBCT₁₈, indicating no

significant difference between micro-CT and each CBCT scan. There was a trend toward overestimation of volume in the CBCT₁₈ scan, but it was not significant.

Similarly, studies by Shaheen et al. and Ye et al. found an increase in volume with increased voxel size. The increased volume could be contributed to increased partial volume artifacts, inconsistency in root canal segmentation, or operator skill.^{2,14} A study by Wang et al. reported good agreement between CBCT 125 μm and micro-CT, without additional information of over- or underestimation trends.⁴

This is in contrast to several studies by Maret et al., which examined the relationship between micro-CT and various CBCT resolutions (ranging from 76 μm to 300 μm). Although the difference in volume was not statistically significant, there was a trend toward underestimation of volume with increased voxel size. This underestimation of volume and associated qualitative and quantitative differences became significant with voxels sizes of 300 μm and above.¹⁸⁻²⁰

Voxel Count

In the current study, a smaller voxel count was associated with increased voxel size. There are few, if any, studies that specifically examine voxel count and its relationship to 3D imaging and reconstruction. However, voxel size can have clinically significant effects the final reconstructed image. Smaller voxel sizes may show increased noise while larger voxel sizes are more prone to partial volume effect and the resultant disappearance of structures.^{2,21}

Length

Consistency in length was seen among all groups in the current study. The micro-CT values were slightly longer than the CBCT values, but no clinical or statistical significance was confirmed. The increased ease of visualization and segmentation of higher resolution scans may have contributed to the increased micro-CT values. The results of this study correspond to similar studies on linear measurements. Studies have shown linear CBCT measurements to have a high degree of accuracy resulting in a 1:1 ratio.^{7,25} The ability to easily and accurately determine length may be beneficial in future studies when evaluating apical root resorption or in calculating root volume.

Grayscale Values

The grayscale values in the current study show an increase between micro-CT and CBCT. However, the larger FOV CBCT₁₈ grayscale values were slightly smaller than the CBCT₁₂ values. This could be due to the exo-mass effect, which results when objects outside the FOV influence the gray values within the FOV.^{22,23} Additionally, the SafeBeam™ technology inherent in the NewTom™ 5G unit may have an effect on the grayscale values. This technology is calibrated for human beings, using it with inanimate objects with varying densities may confuse the system; possibly related to the difference in the beam attenuation measured from that of expected values.

A study by Taylor et al. examined the effect of scan resolution on grayscale parameters, and found conflicting data. Voxel sizes similar to those used in the current study were examined, and the gray level histograms were similar for both micro-CT and CBCT. One possible reason for the discrepancy could be different scan times used in the

Taylor et al. study (26.9 s for 200 μm and 8.9 s for 300 μm vs. 26 s in the current study).²⁴ The disparity could also be due to the object being examined. Teeth have several hard tissues of varying density while bone is more uniform and may not be affected by partial volume averaging in the same manner.

Additionally, the inherent image processing of the NewTom™ 5G CBCT scanner used in current study could have an additional effect on the grayscale values from that previously mentioned. This scanner receives data as 14-bit grayscale (16,384 shades of gray), the same as the micro-CT scanner used, however, it exports the data as 16-bit grayscale (65,536 shades of gray).

Effect of Interpolation Approaches

Two interpolation methods, 3D Wrap and Interpolation Toolbox, were assessed in this study. Based upon clinical and statistical findings, it was determined that the Interpolation Toolbox approach provided a more accurate interpolation of the missing data than the 3D Wrap. The 3D Wrap approach smoothed the surface, while filling in missing data. This approach provides an esthetic image, however this interpolation is inconsistent, sometimes overestimating, while underestimating at other times. In the current study there was a significant difference in length with 3D Wrap interpolation from relocation of the apex due to shrinkage. The Interpolation Toolbox approach is a true interpolation method. It has no effect on the unreduced crown structure, and does not provide any smoothing of the mask. This approach maintains the surface irregularities, leaving a “bumpy” surface.

Reliability

Segmentation can be a difficult process to master due to numerous variables that can affect accuracy and reliability. As such, it is important to evaluate intra- and inter-examiner reproducibility. High intraexaminer reliability may be attributed to the ease of thresholding due to individually scanned teeth, rather than within adjacent alveolar bone as would be experienced with a patient volume.

Limitations of the Study and Recommendations for Future Studies

The most conspicuous limitation of the current study was sample size. The sample consisted of five single-rooted teeth. Initial power calculations estimated a sample size of sixteen for adequate analysis. However, due to unforeseen circumstances, less than one-third of the recommended sample size was evaluated. Another possible limitation, related to tooth selection, is the lack of multi-rooted teeth. Although anterior and posterior teeth were included, all were single-rooted with similar conical root structure, lacking concavities and irregularities.

Another prominent limitation of this study involved software capability. During the course of this study, deficiencies in the ability of the software to accurately measure surface area, predict tooth shape along a curve, interpolate data that was smaller than five voxels, and define the parameters by which the 3D wrap function smoothes a mask, were encountered.

Furthermore, the file formats differed between micro-CT and CBCT scans (BMP vs. DICOM, respectively). It is unknown if the difference in file format affected the

measurements, or if any degradation of data occurred upon being imported into Simpleware™ ScanIP.

Additional inconsistencies may have been introduced through two different examiners positioning the teeth and performing the scans, and differing levels of experience between the two examiners. An employee of the Loma Linda University Center for Dental Research performed the micro-CT scans, while the examiner of the current study performed the CBCT₁₂ and CBCT₁₈ scans. There is noticeable noise in the CBCT₁₂ scan (Figure 3) that is not apparent in the micro-CT or CBCT₁₈ scans. The exact cause of this is unknown, but could be due to a difference in filters applied unknowingly during reconstruction of the CBCT scans.

Finally, this study examined individually scanned, extracted teeth. Manipulation of individual teeth provides greater ease of thresholding and segmentation. However, this does not accurately represent a clinical environment. In clinical practice, teeth are within alveolar bone, adding an additional element of difficulty to segmentation, and possibly decreasing measurement accuracy depending upon artifacts present in the scan, and operator proficiency in segmentation.

Conclusions

1. Due to the small sample size, and statistically significant difference in overall mean volume between micro-CT and CBCT, it cannot be concluded that micro-CT and CBCT scans produce the same volume, and the null must be rejected.
2. It can be concluded that the 3D wrap approach does not provide an accurate interpolation of tooth structure and would not be reliable in a clinical setting for

assessment of tooth volume. The Interpolation Toolbox approach, however, does provide adequate interpolation of tooth structure and would be recommended for use in a clinical setting for assessment of tooth volume.

References

1. Palomo JM, Rao PS, Hans MG. Influence of CBCT exposure conditions on radiation dose. *Oral Surg Oral Med Oral Pathol Oral Radiol Endod* 2008;105:773-782.
2. Ye N, Jian F, Xue J, Wang S, Liao L, Huang W et al. Accuracy of in-vitro tooth volumetric measurements from cone-beam computed tomography. *Am J Orthod Dentofacial Orthop* 2012;142:879-887.
3. Ponder SN, Benavides E, Kapila S, Hatch NE. Quantification of external root resorption by low- vs high-resolution cone-beam computed tomography and periapical radiography: A volumetric and linear analysis. *Am J Orthod Dentofacial Orthop* 2013;143:77-91.
4. Wang Y, He S, Yu L, Li J, Chen S. Accuracy of volumetric measurement of teeth in vivo based on cone beam computer tomography. *Orthod Craniofac Res* 2011;14:206-212.
5. Machado GL. CBCT imaging - A boon to orthodontics. *Saudi Dent J* 2015;27:12-21.
6. Periago DR, Scarfe WC, Moshiri M, Scheetz JP, Silveira AM, Farman AG. Linear accuracy and reliability of cone beam CT derived 3-dimensional images constructed using an orthodontic volumetric rendering program. *Angle Orthod* 2008;78:387-395.
7. Lagravère MO, Carey J, Toogood RW, Major PW. Three-dimensional accuracy of measurements made with software on cone-beam computed tomography images. *Am J Orthod Dentofac Orthop* 2008;134:112-116.
8. Venkatesh E, Elluru SV. Cone beam computed tomography: basics and applications in dentistry. *Journal of Istanbul University Fac Dent* 2017;51:S102-S121.
9. Sunil G, Ram RS, & Ranganayakulu I. CBCT: A swap to conventional orthodontic imaging. *Journal of Dr. NTR University of Health Sciences* 2018;7:85-88.
10. Liu Y, Olszewski R, Alexandroni ES, Enciso R, Xu T, Mah JK. The validity of in vivo tooth volume determinations from cone-beam computed tomography. *Angle Orthod* 2010;80:160-166.
11. Sang YH, Hu HC, Lu SH, Wu YW, Li WR, Tang ZH. Accuracy assessment of three-dimensional surface reconstructions of in vivo teeth from cone-beam computed tomography. *Chin Med J (Engl)* 2016;129:1464-1470.
12. Weissheimer A, Menezes LM, Sameshima GT, Enciso R, Pham J, Grauer D. Imaging software accuracy for 3-dimensional analysis of the upper airway. *Am J Orthod Dentofacial Orthop* 2012;142:801-813.

13. Bhargavi K, Jyothi, S. A Survey on threshold based segmentation technique in image processing. *Int J Innov Res Dev* 2014;3:234-239.
14. Shaheen E, Khali W, Ezeldeen M, Castele EV, Su Y, Politis C, Jacobs R. Accuracy of segmentation of tooth structures using 3 different CBCT machines. *Oral Surg, Oral Med, Oral Path and Oral Radiol* 2017;123:123-128.
15. Forst D, Nijar S, Flores-Mir C, Carey J, Secanell M, Lagravere M. Comparison of in vivo 3D cone-beam computed tomography tooth volume measurement protocols. *Prog Orthod* 2014;15:1-13.
16. Mah JK, Yi L, Huang RC, Choo H. Advanced applications of cone beam computed tomography in orthodontics. *Semin Orthod* 2011;17:57-71.
17. Jheo AH, Obero S, Solem RC, Kapila S. Moving towards precision orthodontics: An evolving paradigm shift in the planning and delivery of customized orthodontic therapy. *Orthod Craniofac Res* 2017;20:106-113.
18. Maret D, Telmon N, Peters OA, Lepage B, Treil J, Inglessè JM, Peyre A, Kahn JL, Sixou M. Effect of voxel size on the accuracy of 3D reconstructions with cone beam CT. *Dentomaxillofac Radiol* 2012;41:649-655.
19. Maret D, Peters OA, Galibourg A, Dumoncel J, Esclassan R, Kahn J, Sixou M, Telmon N. Comparison of the accuracy of 3-dimensional cone-beam computed tomography and micro-computed tomography reconstructions by using different voxel sizes. *J Endod* 2014;40:1321-1326.
20. Maret D, Molinier F, Braga J, Peters OA, Telmon N, Treil J, Inglessè JM, Cossìé A, Kahn JL, Sixou M. Accuracy of 3D reconstructions based on cone beam computed tomography. *J Dent Res* 2010;89:1465-1469.
21. Spin-Neto R, Gotfredsen, E, Wenzel A. Impact of voxel size variation on CBCT-based diagnostic outcomes in dentistry: a systematic review. *J Digit Imag* 2013;26:813-820.
22. Birur N, Patrick S, Gurushanth K, Raghavan A, Gurudath S. Comparison of gray values of cone-beam computed tomography with hounsfield units of multislice computed tomography: An in vitro study. *Indian J Dent Res* 2017;28:66-70.
23. Pauwels R, Nackaerts O, Bellaiche N, Stamatakis H, Tsiklakis K, Walker A, Bosmans H, Bogaerts R, Jacobs R, Horner K. Variability of dental cone beam CT grey values for density estimations. *B J Radiol* 2013; 86: 20120135(1-9)
24. Taylor T, Gans S, Jones E, Firestone A, Johnston W, Kim D. Comparison of micro-CT and cone beam CT-based assessments for relative difference of grey level distribution in a human mandible. *Dentomaxillofac Radiol* 2013; 42:25117764(1-8)

25. Sherrard JF, Rossouw PE, Benson BW, Carrillo R, Buschang PH. Accuracy and reliability of tooth and root lengths measured on cone-beam computed tomographs. *Am J Orthod Dentofacial Orthop* 2010;137:S100-108.
26. Mozzo P, Procacci C, Tacconi A, Martini PT, Andreis IA. A new volumetric CT machine for dental imaging based on the cone-beam technique: preliminary results. *Eur Radiol* 1998;8:1558-1564.
27. Silva MA, Wolf U, Heinicke F, Bumann A, Visser H, Hirsch E. Cone-beam computed tomography for routine orthodontic treatment planning: a radiation dose evaluation. *Am J Orthod Dentofacial Orthop* 2008;133:640.e1-5.
28. Scarfe WC, Farman AG. *Cone-Beam Computed Tomography Oral Radiology: Principles and Interpretation*. 6th ed. St. Louis, MO: Mosby Elsevier; 2009. p. 225-243.
29. Hatcher DC. *Operational Principles for Cone-Beam Computed Tomography*. The J Am Dent Assoc 2010;141:3S-6S.
30. Ludlow JB, Davies-Ludlow LE, White SC. Patient Risk Related to Common Dental Radiographic Examinations. *J Am Dent Assoc* 2008;139:1237-1243.
31. White SC, Pharoah MJ. *Radiation Safety and Protection Oral Radiology: Principles and Interpretation*. 6th ed. St. Louis, MO: Mosby Elsevier; 2009. p. 32-43.
32. Campos MJ, Silva KS, Gravina MA, Fraga MR, Vitral RW. Apical root resorption: the dark side of the root. *Am J Orthod Dentofacial Orthop* 2013;143:492-498.
33. Grauer D, Cevidanes LS, Proffit WR. Working with DICOM craniofacial images. *Am J Orthod Dentofacial Orthop* 2009;136:460-470.
34. Flint DJ, Velasco RC. Cone beam computed tomography (CBCT) applications in dentistry 2017;5. Retrieved from <https://www.dentalcare.com/en-us/professional-education/ce-courses/ce531/image-acquisition-and-reconstruction>.
35. QR s.r.l.; NewTom™ Giano Version 08-2017. Verona, Italy.
36. Molen AD. Comparing cone beam computed tomography systems from an orthodontic perspective. *Semin Orthod* 2011;17:34-38.
37. Scarfe WC, Farman AG. What is cone-beam CT and how does it work? *Dent Clin North Am* 2008;52:707-730.
38. Farman AG, Scarfe WC. The Basics of maxillofacial cone beam computed tomography. *Semin Orthod* 2009;15:2-13.

39. Brüllmann D, Schulze RK. Spatial resolution in CBCT machines for dental/maxillofacial applications—what do we know today? *Dentomaxillofac Radiol* 2015; 44:20140204(1-8).
40. Peck MT, Gonzalez SM. Interpretation basics of cone beam computed tomography. *Int J Contemp Dent Med Rev* 2015.
41. Schulze R, Heil U, Grob D, Bruellmann DD, Dranischnikow E, Schwanecke U, Schoemer E. Artifacts in CBCT: a review. *Dentomaxillofac Radiol* 2011;40:265-273.
42. Abramovitch K, Rice DD. Basic Principles of cone beam computed tomography. *Dent Clin North Am* 2014;58:463-484.
43. Synopsys, Inc. Simpleware™ ScanIP: Tutorial Guide Version 2016.09-SP1. Mountain View, CA.
44. Wierzbicki T, El-Bialy T, Aldaghreer S, Li G, Doschak M. Analysis of orthodontically induced root resorption using micro-computed tomography (Micro-CT). *Angle Orthod* 2009;79:91-96.

CHAPTER THREE

DISCUSSION

Extended Discussion

CBCT technology was introduced into the field of dentistry nearly two decades ago. Since then, widespread application of this technology has made CBCT an integral part of diagnosis and treatment planning in all areas of dentistry, especially orthodontics. Ease of use and diagnostic accuracy have allowed for rapid adoption of this imaging modality.²³ Despite the years of innovation, there are still areas of CBCT data manipulation that have yet to be explored.

3D virtual treatment planning, although rooted in the gross orthopedic movements of surgical planning, has the ability to simulate virtual orthodontic movements. These fine movements based upon biomechanical methods of tooth movement have not been thoroughly explored. Companies like SureSmile[®] (OraMetrix; Richardson, TX, USA) and Insignia[®] (Ormco; Orange County, CA, USA) allow for customized brackets and archwires based upon final tooth positions derived from CBCT data. Clear aligners may also be customized in a similar way using technology from Orchestrate[®] (Orchestrate3D; www.orchestrate3d.com) and InVivo5[®] (Anatomage). Although these methods use CBCT scans to determine final tooth position, they do not know the exact force required to get the tooth to that final position.¹⁷

Future Studies

A study by Maret et al. investigated the differences in reconstructed surfaces of micro-CT and CBCT scans. There was no significant difference between 3D

reconstructed surface structures, leaving one to imply that surface area and volume could be accurately calculated from CBCT scans.²⁰ This has great significance for the field of dentistry, specifically the orthodontic realm. Knowledge of the volume and/or surface area of the root would be beneficial to aid in determination of force values for efficient tooth movement.

CBCT imaging is thought to provide superior visualization of alveolar bone height and surface irregularities, as well as accurate assessment of bone mineralization based upon grayscale values.^{16,24} Likewise, the ability to accurately reconstruct surface structures as discussed above, combined with adequate estimation of bone density based upon grayscale values, may allow for calculation of bone volume. Familiarity with the volume of bone surrounding a tooth, the surface area of a tooth, and the forces required for tooth movement may lead to more efficient treatment and shortened treatment times.

APPENDIX A

RAW DATA

Maxillary Right Lateral Incisor

| TRIAL 1 | | Volume | | | Length | | | Voxel Count | | | Grayscale Values | | |
|------------------------------|----------|----------|----------|----------|----------|----------|----------|-------------|--------|----------|------------------|----------|--|
| Reduction | Micro-CT | CBCT12 | CBCT18 | Micro-CT | CBCT12 | CBCT18 | Micro-CT | CBCT12 | CBCT18 | Micro-CT | CBCT12 | CBCT18 | |
| 100% | 3.51E+02 | 3.48E+02 | 3.68E+02 | 2.36E+01 | 2.35E+01 | 2.36E+01 | 18882644 | 177961 | 13629 | 1.59E+02 | 2.29E+03 | 1.81E+03 | |
| 50% | | 2.68E+02 | 2.86E+02 | | 2.35E+01 | 2.36E+01 | | 137166 | 10587 | | 2.32E+03 | 1.83E+03 | |
| 25% | | 2.28E+02 | 2.45E+02 | | 2.35E+01 | 2.36E+01 | | 116822 | 9067 | | 2.34E+03 | 1.85E+03 | |
| 12.50% | | 2.08E+02 | 2.24E+02 | | 2.35E+01 | 2.35E+01 | | 106619 | 8294 | | 2.35E+03 | 1.86E+03 | |
| 6.25% | | 1.98E+02 | 2.14E+02 | | 2.35E+01 | 2.35E+01 | | 101529 | 7928 | | 2.36E+03 | 1.86E+03 | |
| CEJ, Midroot, Apex | | 1.92E+02 | 2.12E+02 | | 2.35E+01 | 2.35E+01 | | 98102 | 7836 | | 2.37E+03 | 1.86E+03 | |
| 3D Wrap Interpolation | | | | | | | | | | | | | |
| 100% | 3.86E+02 | 3.41E+02 | 2.40E+02 | 2.36E+01 | 2.28E+01 | 2.05E+01 | 20729806 | 174509 | 8906 | 1.49E+02 | 2.25E+03 | 1.84E+03 | |
| 50% | | 3.43E+02 | 2.66E+02 | | 2.31E+01 | 2.12E+01 | | 175661 | 9842 | | 2.25E+03 | 1.84E+03 | |
| 25% | | 3.41E+02 | 2.64E+02 | | 2.31E+01 | 2.16E+01 | | 174517 | 9760 | | 2.25E+03 | 1.84E+03 | |
| 12.50% | | 3.41E+02 | 2.52E+02 | | 2.30E+01 | 2.13E+01 | | 174744 | 9322 | | 2.25E+03 | 1.85E+03 | |
| 6.25% | | 3.40E+02 | 2.42E+02 | | 2.30E+01 | 2.13E+01 | | 174314 | 8967 | | 2.25E+03 | 1.84E+03 | |
| CEJ, Midroot, Apex | | 3.26E+02 | 2.00E+02 | | 2.28E+01 | 1.86E+01 | | 166860 | 7414 | | 2.25E+03 | 1.81E+03 | |
| Interpolation Toolbox | | | | | | | | | | | | | |
| 100% | | | | | 2.47E+01 | 2.36E+01 | | 178161 | 13637 | | 2.29E+03 | 1.81E+03 | |
| 50% | | 3.48E+02 | 3.68E+02 | | 2.36E+01 | 2.36E+01 | | 178002 | 13659 | | 2.29E+03 | 1.81E+03 | |
| 25% | | 3.48E+02 | 3.69E+02 | | 2.36E+01 | 2.36E+01 | | 177646 | 13607 | | 2.29E+03 | 1.81E+03 | |
| 12.50% | | 3.47E+02 | 3.67E+02 | | 2.36E+01 | 2.36E+01 | | 176792 | 13385 | | 2.29E+03 | 1.82E+03 | |
| 6.25% | | 3.45E+02 | 3.61E+02 | | 2.35E+01 | 2.36E+01 | | 163745 | 12893 | | 2.32E+03 | 1.83E+03 | |
| CEJ, Midroot, Apex | | 3.20E+02 | 3.48E+02 | | 2.35E+01 | 2.36E+01 | | | | | | | |
| TRIAL 2 | | | | | | | | | | | | | |
| TRIAL 2 | | Volume | | | Length | | | Voxel Count | | | Grayscale Values | | |
| Reduction | Micro-CT | CBCT12 | CBCT18 | Micro-CT | CBCT12 | CBCT18 | Micro-CT | CBCT12 | CBCT18 | Micro-CT | CBCT12 | CBCT18 | |
| 100% | 3.51E+02 | 3.35E+02 | 3.51E+02 | 2.36E+01 | 2.35E+01 | 2.34E+01 | 18882674 | 171736 | 12997 | 1.59E+02 | 2.32E+03 | 1.85E+03 | |
| 50% | | 2.58E+02 | 2.73E+02 | | 2.35E+01 | 2.34E+01 | | 132193 | 10119 | | 2.35E+03 | 1.87E+03 | |
| 25% | | 2.20E+02 | 2.35E+02 | | 2.35E+01 | 2.34E+01 | | 112411 | 8698 | | 2.37E+03 | 1.89E+03 | |
| 12.50% | | 2.00E+02 | 2.15E+02 | | 2.34E+01 | 2.33E+01 | | 102479 | 7974 | | 2.38E+03 | 1.90E+03 | |
| 6.25% | | 1.91E+02 | 2.06E+02 | | 2.34E+01 | 2.33E+01 | | 97536 | 7630 | | 2.39E+03 | 1.90E+03 | |
| CEJ, Midroot, Apex | | 1.84E+02 | 2.04E+02 | | 2.34E+01 | 2.33E+01 | | 94202 | 7543 | | 2.40E+03 | 1.90E+03 | |
| 3D Wrap Interpolation | | | | | | | | | | | | | |
| 100% | 3.87E+02 | 3.33E+02 | 2.38E+02 | 2.36E+01 | 2.28E+01 | 2.03E+01 | 20796886 | 170441 | 8822 | 1.48E+02 | 2.26E+03 | 1.88E+03 | |
| 50% | | 3.36E+02 | 2.67E+02 | | 2.31E+01 | 2.16E+01 | | 172111 | 9874 | | 2.26E+03 | 1.86E+03 | |
| 25% | | 3.37E+02 | 2.64E+02 | | 2.31E+01 | 2.15E+01 | | 172455 | 9763 | | 2.25E+03 | 1.86E+03 | |
| 12.50% | | 3.36E+02 | 2.59E+02 | | 2.30E+01 | 2.14E+01 | | 172061 | 9596 | | 2.25E+03 | 1.87E+03 | |
| 6.25% | | 3.29E+02 | 2.46E+02 | | 2.29E+01 | 2.14E+01 | | 168568 | 9122 | | 2.27E+03 | 1.86E+03 | |
| CEJ, Midroot, Apex | | 2.91E+02 | 2.18E+02 | | 2.21E+01 | 1.97E+01 | | 149092 | 8068 | | 2.26E+03 | 1.87E+03 | |
| Interpolation Toolbox | | | | | | | | | | | | | |
| 100% | | | | | 2.35E+01 | 2.34E+01 | | 172371 | 12977 | | 2.32E+03 | 1.85E+03 | |
| 50% | | 3.37E+02 | 3.50E+02 | | 2.35E+01 | 2.34E+01 | | 172085 | 12977 | | 2.32E+03 | 1.85E+03 | |
| 25% | | 3.36E+02 | 3.50E+02 | | 2.35E+01 | 2.34E+01 | | 171263 | 12983 | | 2.32E+03 | 1.85E+03 | |
| 12.50% | | 3.34E+02 | 3.51E+02 | | 2.35E+01 | 2.34E+01 | | 170082 | 12727 | | 2.32E+03 | 1.86E+03 | |
| 6.25% | | 3.32E+02 | 3.44E+02 | | 2.35E+01 | 2.34E+01 | | 157650 | 12481 | | 2.34E+03 | 1.86E+03 | |
| CEJ, Midroot, Apex | | 3.08E+02 | 3.37E+02 | | 2.35E+01 | 2.34E+01 | | | | | | | |
| TRIAL 3 | | | | | | | | | | | | | |
| TRIAL 3 | | Volume | | | Length | | | Voxel Count | | | Grayscale Values | | |
| Reduction | Micro-CT | CBCT12 | CBCT18 | Micro-CT | CBCT12 | CBCT18 | Micro-CT | CBCT12 | CBCT18 | Micro-CT | CBCT12 | CBCT18 | |
| 100% | 3.51E+02 | 3.36E+02 | 3.38E+02 | 2.36E+01 | 2.35E+01 | 2.33E+01 | 18882668 | 171739 | 12517 | 1.59E+02 | 2.32E+03 | 1.88E+03 | |
| 50% | | 2.57E+02 | 2.61E+02 | | 2.35E+01 | 2.33E+01 | | 132194 | 9664 | | 2.35E+03 | 1.90E+03 | |
| 25% | | 2.21E+02 | 2.23E+02 | | 2.35E+01 | 2.33E+01 | | 112411 | 8242 | | 2.37E+03 | 1.92E+03 | |
| 12.50% | | 2.01E+02 | 2.03E+02 | | 2.34E+01 | 2.33E+01 | | 102479 | 7532 | | 2.38E+03 | 1.92E+03 | |
| 6.25% | | 1.91E+02 | 1.94E+02 | | 2.34E+01 | 2.33E+01 | | 97537 | 7187 | | 2.39E+03 | 1.93E+03 | |
| CEJ, Midroot, Apex | | 1.85E+02 | 1.92E+02 | | 2.34E+01 | 2.32E+01 | | 94192 | 7094 | | 2.40E+03 | 1.93E+03 | |
| 3D Wrap Interpolation | | | | | | | | | | | | | |
| 100% | 3.87E+02 | 3.33E+02 | 2.48E+02 | 2.36E+01 | 2.28E+01 | 2.04E+01 | 20796886 | 170441 | 9179 | 1.48E+02 | 2.26E+03 | 1.86E+03 | |
| 50% | | 3.36E+02 | 2.65E+02 | | 2.31E+01 | 2.15E+01 | | 172111 | 9808 | | 2.26E+03 | 1.88E+03 | |
| 25% | | 3.37E+02 | 2.65E+02 | | 2.31E+01 | 2.15E+01 | | 172455 | 9797 | | 2.25E+03 | 1.88E+03 | |
| 12.50% | | 3.36E+02 | 2.57E+02 | | 2.30E+01 | 2.11E+01 | | 172061 | 9525 | | 2.25E+03 | 1.89E+03 | |
| 6.25% | | 3.29E+02 | 2.36E+02 | | 2.29E+01 | 2.11E+01 | | 168568 | 8735 | | 2.27E+03 | 1.90E+03 | |
| CEJ, Midroot, Apex | | 2.91E+02 | 2.00E+02 | | 2.21E+01 | 1.87E+01 | | 149092 | 7392 | | 2.26E+03 | 1.86E+03 | |
| Interpolation Toolbox | | | | | | | | | | | | | |
| 100% | | | | | 2.35E+01 | 2.33E+01 | | 172371 | 12483 | | 2.32E+03 | 1.88E+03 | |
| 50% | | 3.36E+02 | 3.37E+02 | | 2.35E+01 | 2.33E+01 | | 172085 | 12497 | | 2.32E+03 | 1.88E+03 | |
| 25% | | 3.36E+02 | 3.37E+02 | | 2.35E+01 | 2.33E+01 | | 171263 | 12488 | | 2.32E+03 | 1.88E+03 | |
| 12.50% | | 3.34E+02 | 3.37E+02 | | 2.35E+01 | 2.33E+01 | | 170082 | 12334 | | 2.32E+03 | 1.88E+03 | |
| 6.25% | | 3.32E+02 | 3.33E+02 | | 2.35E+01 | 2.33E+01 | | 157650 | 11905 | | 2.34E+03 | 1.89E+03 | |
| CEJ, Midroot, Apex | | 3.08E+02 | 3.21E+02 | | 2.35E+01 | 2.33E+01 | | | | | | | |

Maxillary Left Canine

| TRIAL 1 | | | Volume | | | Length | | | Voxel Count | | | Grayscale Values | | |
|------------------------------|----------|----------|----------|----------|----------|----------|----------|--------|-------------|----------|----------|------------------|--|--|
| Reduction | Micro-CT | CBCT12 | CBCT18 | Micro-CT | CBCT12 | CBCT18 | Micro-CT | CBCT12 | CBCT18 | Micro-CT | CBCT12 | CBCT18 | | |
| 100% | 6.74E+02 | 6.71E+02 | 6.99E+02 | 2.92E+01 | 2.90E+01 | 2.89E+01 | 36214142 | 343454 | 25879 | 1.50E+02 | 2.26E+03 | 2.53E+03 | | |
| 50% | | 4.82E+02 | 5.09E+02 | | 2.90E+01 | 2.89E+01 | | 246983 | 18850 | | 2.29E+03 | 2.63E+03 | | |
| 25% | | 3.88E+02 | 4.15E+02 | | 2.90E+01 | 2.89E+01 | | 198897 | 15362 | | 2.31E+03 | 2.72E+03 | | |
| 12.50% | | 3.41E+02 | 3.67E+02 | | 2.90E+01 | 2.89E+01 | | 174751 | 13592 | | 2.32E+03 | 2.78E+03 | | |
| 6.25% | | 3.18E+02 | 3.44E+02 | | 2.91E+01 | 2.90E+01 | | 162830 | 12727 | | 2.33E+03 | 2.81E+03 | | |
| CEJ, Midroot, Apex | | 2.99E+02 | 3.33E+02 | | 2.89E+01 | 2.89E+01 | | 153240 | 12315 | | 2.34E+03 | 2.83E+03 | | |
| 3D Wrap Interpolation | | | | | | | | | | | | | | |
| 100% | 7.07E+02 | 6.71E+02 | 5.25E+02 | 2.92E+01 | 2.84E+01 | 2.58E+01 | 38017925 | 343656 | 19436 | 1.46E+02 | 2.20E+03 | 2.61E+03 | | |
| 50% | | 6.69E+02 | 5.74E+02 | | 2.85E+01 | 2.72E+01 | | 342552 | 21268 | | 2.22E+03 | 2.57E+03 | | |
| 25% | | 6.66E+02 | 5.78E+02 | | 2.85E+01 | 2.72E+01 | | 341238 | 21398 | | 2.22E+03 | 2.56E+03 | | |
| 12.50% | | 6.66E+02 | 5.80E+02 | | 2.85E+01 | 2.71E+01 | | 340967 | 21470 | | 2.22E+03 | 2.55E+03 | | |
| 6.25% | | 6.67E+02 | 5.67E+02 | | 2.85E+01 | 2.71E+01 | | 341547 | 21014 | | 2.22E+03 | 2.56E+03 | | |
| CEJ, Midroot, Apex | | 6.11E+02 | 5.26E+02 | | 2.83E+01 | 2.65E+01 | | 312649 | 19499 | | 2.24E+03 | 2.58E+03 | | |
| Interpolation Toolbox | | | | | | | | | | | | | | |
| 100% | | | | | | | | | | | | | | |
| 50% | | 6.72E+02 | 6.99E+02 | | 2.90E+01 | 2.89E+01 | | 343869 | 25891 | | 2.26E+03 | 2.53E+03 | | |
| 25% | | 6.72E+02 | 7.00E+02 | | 2.90E+01 | 2.89E+01 | | 343978 | 25931 | | 2.25E+03 | 2.53E+03 | | |
| 12.50% | | 6.71E+02 | 6.99E+02 | | 2.90E+01 | 2.89E+01 | | 343395 | 25904 | | 2.26E+03 | 2.52E+03 | | |
| 6.25% | | 6.71E+02 | 6.96E+02 | | 2.90E+01 | 2.89E+01 | | 343394 | 25795 | | 2.25E+03 | 2.52E+03 | | |
| CEJ, Midroot, Apex | | 6.18E+02 | 6.70E+02 | | 2.90E+01 | 2.89E+01 | | 316315 | 24816 | | 2.27E+03 | 2.55E+03 | | |

| TRIAL 2 | | | Volume | | | Length | | | Voxel Count | | | Grayscale Values | | |
|------------------------------|----------|----------|----------|----------|----------|----------|----------|--------|-------------|----------|----------|------------------|--|--|
| Reduction | Micro-CT | CBCT12 | CBCT18 | Micro-CT | CBCT12 | CBCT18 | Micro-CT | CBCT12 | CBCT18 | Micro-CT | CBCT12 | CBCT18 | | |
| 100% | 6.74E+02 | 6.36E+02 | 6.05E+02 | 2.92E+01 | 2.90E+01 | 2.85E+01 | 36213407 | 325624 | 22400 | 1.50E+02 | 2.31E+03 | 2.69E+03 | | |
| 50% | | 4.58E+02 | 4.49E+02 | | 2.90E+01 | 2.85E+01 | | 234689 | 16620 | | 2.33E+03 | 2.78E+03 | | |
| 25% | | 3.70E+02 | 3.71E+02 | | 2.90E+01 | 2.85E+01 | | 189387 | 13725 | | 2.35E+03 | 2.86E+03 | | |
| 12.50% | | 3.25E+02 | 3.31E+02 | | 2.90E+01 | 2.85E+01 | | 166647 | 12269 | | 2.37E+03 | 2.91E+03 | | |
| 6.25% | | 3.03E+02 | 3.12E+02 | | 2.90E+01 | 2.85E+01 | | 155360 | 11549 | | 2.38E+03 | 2.94E+03 | | |
| 3.125% | | 2.92E+02 | 3.02E+02 | | 2.90E+01 | 2.85E+01 | | 149717 | 11180 | | 2.38E+03 | 2.96E+03 | | |
| CEJ, Midroot, Apex | | 2.86E+02 | 3.03E+02 | | 2.88E+01 | 2.85E+01 | | 146463 | 11222 | | 2.38E+03 | 2.96E+03 | | |
| 3D Wrap Interpolation | | | | | | | | | | | | | | |
| 100% | 7.07E+02 | 6.66E+02 | 4.83E+02 | 2.92E+01 | 2.83E+01 | 2.48E+01 | 37978911 | 341056 | 17900 | 1.46E+02 | 2.22E+03 | 2.60E+03 | | |
| 50% | | 6.47E+02 | 4.92E+02 | | 2.85E+01 | 2.64E+01 | | 331519 | 18235 | | 2.25E+03 | 2.62E+03 | | |
| 25% | | 6.45E+02 | 4.94E+02 | | 2.85E+01 | 2.61E+01 | | 330416 | 18279 | | 2.25E+03 | 2.61E+03 | | |
| 12.50% | | 6.45E+02 | 4.94E+02 | | 2.85E+01 | 2.63E+01 | | 330022 | 18304 | | 2.25E+03 | 2.61E+03 | | |
| 6.25% | | 6.43E+02 | 4.74E+02 | | 2.85E+01 | 2.63E+01 | | 329383 | 17560 | | 2.25E+03 | 2.61E+03 | | |
| 3.125% | | 6.42E+02 | 3.13E+02 | | 2.85E+01 | 2.24E+01 | | 328539 | 11599 | | 2.25E+03 | 2.45E+03 | | |
| CEJ, Midroot, Apex | | 5.99E+02 | 4.44E+02 | | 2.83E+01 | 2.54E+01 | | 306639 | 16434 | | 2.26E+03 | 2.62E+03 | | |
| Interpolation Toolbox | | | | | | | | | | | | | | |
| 100% | | | | | | | | | | | | | | |
| 50% | | 6.35E+02 | 6.02E+02 | | 2.90E+01 | 2.85E+01 | | 324982 | 22287 | | 2.30E+03 | 2.69E+03 | | |
| 25% | | 6.40E+02 | 6.02E+02 | | 2.90E+01 | 2.85E+01 | | 327915 | 22290 | | 2.30E+03 | 2.69E+03 | | |
| 12.50% | | 6.39E+02 | 6.01E+02 | | 2.90E+01 | 2.85E+01 | | 327190 | 22260 | | 2.30E+03 | 2.69E+03 | | |
| 6.25% | | 6.37E+02 | 5.94E+02 | | 2.90E+01 | 2.85E+01 | | 326028 | 22004 | | 2.29E+03 | 2.69E+03 | | |
| 3.125% | | 6.27E+02 | 5.74E+02 | | 2.90E+01 | 2.85E+01 | | 320944 | 21241 | | 2.29E+03 | 2.71E+03 | | |
| CEJ, Midroot, Apex | | 5.71E+02 | 5.77E+02 | | 2.90E+01 | 2.85E+01 | | 292498 | 21363 | | 2.30E+03 | 2.70E+03 | | |

| TRIAL 3 | | | Volume | | | Length | | | Voxel Count | | | Grayscale Values | | |
|------------------------------|----------|----------|----------|----------|----------|----------|----------|--------|-------------|----------|----------|------------------|--|--|
| Reduction | Micro-CT | CBCT12 | CBCT18 | Micro-CT | CBCT12 | CBCT18 | Micro-CT | CBCT12 | CBCT18 | Micro-CT | CBCT12 | CBCT18 | | |
| 100% | 6.74E+02 | 6.42E+02 | 6.86E+02 | 2.92E+01 | 3.14E+01 | 2.89E+01 | 36214142 | 325615 | 25425 | 1.50E+02 | 2.31E+03 | 2.55E+03 | | |
| 50% | | 4.70E+02 | 5.01E+02 | | 2.90E+01 | 2.89E+01 | | 234692 | 18559 | | 2.33E+03 | 2.65E+03 | | |
| 25% | | 3.82E+02 | 4.09E+02 | | 2.90E+01 | 2.89E+01 | | 189427 | 15155 | | 2.35E+03 | 2.74E+03 | | |
| 12.50% | | 3.37E+02 | 3.62E+02 | | 2.90E+01 | 2.89E+01 | | 166653 | 13425 | | 2.37E+03 | 2.80E+03 | | |
| 6.25% | | 3.15E+02 | 3.40E+02 | | 2.90E+01 | 2.89E+01 | | 155353 | 12583 | | 2.38E+03 | 2.83E+03 | | |
| 3.125% | | 2.99E+02 | 3.28E+02 | | 2.90E+01 | 2.89E+01 | | 149715 | 12140 | | 2.38E+03 | 2.85E+03 | | |
| CEJ, Midroot, Apex | | 2.88E+02 | 3.29E+02 | | 2.88E+01 | 2.89E+01 | | 146461 | 12185 | | 2.38E+03 | 2.85E+03 | | |
| 3D Wrap Interpolation | | | | | | | | | | | | | | |
| 100% | 7.07E+02 | 6.78E+02 | 5.18E+02 | 2.92E+01 | 2.86E+01 | 2.66E+01 | 38017874 | 347353 | 19172 | 1.46E+02 | 2.19E+03 | 2.58E+03 | | |
| 50% | | 6.46E+02 | 5.56E+02 | | 2.85E+01 | 2.72E+01 | | 330759 | 20575 | | 2.25E+03 | 2.57E+03 | | |
| 25% | | 6.44E+02 | 5.56E+02 | | 2.85E+01 | 2.72E+01 | | 329828 | 20580 | | 2.25E+03 | 2.57E+03 | | |
| 12.50% | | 6.43E+02 | 5.57E+02 | | 2.85E+01 | 2.71E+01 | | 329439 | 20623 | | 2.25E+03 | 2.56E+03 | | |
| 6.25% | | 6.43E+02 | 5.50E+02 | | 2.85E+01 | 2.71E+01 | | 329021 | 20388 | | 2.25E+03 | 2.56E+03 | | |
| 3.125% | | 6.41E+02 | 4.08E+02 | | 2.85E+01 | 2.36E+01 | | 328248 | 15120 | | 2.25E+03 | 2.44E+03 | | |
| CEJ, Midroot, Apex | | 5.98E+02 | 5.10E+02 | | 2.83E+01 | 2.65E+01 | | 306401 | 18897 | | 2.26E+03 | 2.57E+03 | | |
| Interpolation Toolbox | | | | | | | | | | | | | | |
| 100% | | | | | | | | | | | | | | |
| 50% | | 6.37E+02 | 6.87E+02 | | 2.90E+01 | 2.89E+01 | | 325898 | 25437 | | 2.30E+03 | 2.55E+03 | | |
| 25% | | 6.40E+02 | 6.87E+02 | | 2.90E+01 | 2.89E+01 | | 327854 | 25429 | | 2.30E+03 | 2.55E+03 | | |
| 12.50% | | 6.39E+02 | 6.87E+02 | | 2.90E+01 | 2.89E+01 | | 326918 | 25428 | | 2.30E+03 | 2.55E+03 | | |
| 6.25% | | 6.37E+02 | 6.84E+02 | | 2.90E+01 | 2.89E+01 | | 326043 | 25317 | | 2.29E+03 | 2.55E+03 | | |
| 3.125% | | 6.27E+02 | 6.54E+02 | | 2.90E+01 | 2.89E+01 | | 320931 | 24218 | | 2.29E+03 | 2.58E+03 | | |
| CEJ, Midroot, Apex | | 5.71E+02 | 6.58E+02 | | 2.90E+01 | 2.89E+01 | | 292496 | 24360 | | 2.30E+03 | 2.57E+03 | | |

Maxillary Left Second Premolar

| TRIAL 1 | | | Volume | | | Length | | | Voxel Count | | | Grayscale Values | | |
|------------------------------|----------|----------|----------|----------|----------|----------|----------|--------|-------------|----------|----------|------------------|--|--|
| Reduction | Micro-CT | CBCT12 | CBCT18 | Micro-CT | CBCT12 | CBCT18 | Micro-CT | CBCT12 | CBCT18 | Micro-CT | CBCT12 | CBCT18 | | |
| 100% | 4.84E+02 | 5.05E+02 | 5.13E+02 | 2.43E+01 | 2.44E+01 | 2.42E+01 | 25983970 | 258487 | 18997 | 1.53E+02 | 3.05E+03 | 2.69E+03 | | |
| 50% | | 3.61E+02 | 3.63E+02 | | 2.44E+01 | 2.42E+01 | | 184880 | 13459 | | 3.18E+03 | 2.80E+03 | | |
| 25% | | 2.89E+02 | 2.90E+02 | | 2.44E+01 | 2.42E+01 | | 148152 | 10730 | | 3.29E+03 | 2.90E+03 | | |
| 12.50% | | 2.53E+02 | 2.52E+02 | | 2.44E+01 | 2.42E+01 | | 129785 | 9338 | | 3.37E+03 | 2.97E+03 | | |
| 6.25% | | 2.35E+02 | 2.34E+02 | | 2.44E+01 | 2.43E+01 | | 120550 | 8680 | | 3.42E+03 | 3.01E+03 | | |
| 3.125% | | 2.26E+02 | 2.25E+02 | | 2.41E+01 | 2.41E+01 | | 115853 | 8320 | | 3.45E+03 | 3.04E+03 | | |
| CEJ, Midroot, Apex | | 2.22E+02 | 2.25E+02 | | 1.82E+01 | 2.40E+01 | | 113433 | 8331 | | 3.47E+03 | 3.04E+03 | | |
| 3D Wrap Interpolation | | | | | | | | | | | | | | |
| 100% | 5.20E+02 | 5.85E+02 | 4.25E+02 | 2.43E+01 | 2.40E+01 | 2.25E+01 | 27962245 | 299485 | 15759 | 1.46E+02 | 2.59E+03 | 2.48E+03 | | |
| 50% | | 5.00E+02 | 3.94E+02 | | 2.41E+01 | 2.31E+01 | | 255851 | 14579 | | 3.01E+03 | 2.74E+03 | | |
| 25% | | 5.00E+02 | 3.89E+02 | | 2.41E+01 | 2.31E+01 | | 255830 | 14390 | | 3.00E+03 | 2.75E+03 | | |
| 12.50% | | 5.02E+02 | 3.86E+02 | | 2.41E+01 | 2.30E+01 | | 256814 | 14292 | | 3.00E+03 | 2.74E+03 | | |
| 6.25% | | 5.04E+02 | 3.82E+02 | | 2.41E+01 | 2.30E+01 | | 258005 | 14154 | | 2.98E+03 | 2.69E+03 | | |
| 3.125% | | 4.98E+02 | 3.47E+02 | | 2.41E+01 | 2.15E+01 | | 255071 | 12865 | | 2.95E+03 | 2.55E+03 | | |
| CEJ, Midroot, Apex | | 4.72E+02 | 3.58E+02 | | 2.39E+01 | 2.27E+01 | | 241588 | 13267 | | 2.87E+03 | 2.60E+03 | | |
| Interpolation Toolbox | | | | | | | | | | | | | | |
| 100% | | | | | | | | | | | | | | |
| 50% | | 5.05E+02 | 5.13E+02 | | 2.44E+01 | 2.42E+01 | | 258325 | 19018 | | 3.05E+03 | 2.69E+03 | | |
| 25% | | 5.04E+02 | 5.15E+02 | | 2.44E+01 | 2.42E+01 | | 258257 | 19071 | | 3.05E+03 | 2.68E+03 | | |
| 12.50% | | 5.04E+02 | 5.13E+02 | | 2.44E+01 | 2.42E+01 | | 258283 | 19011 | | 3.05E+03 | 2.68E+03 | | |
| 6.25% | | 5.03E+02 | 5.17E+02 | | 2.44E+01 | 2.42E+01 | | 257506 | 19143 | | 3.05E+03 | 2.64E+03 | | |
| 3.125% | | 4.94E+02 | 5.03E+02 | | 2.44E+01 | 2.42E+01 | | 253133 | 18617 | | 3.05E+03 | 2.61E+03 | | |
| CEJ, Midroot, Apex | | 4.65E+02 | 4.89E+02 | | 2.44E+01 | 2.42E+01 | | 238095 | 18108 | | 3.01E+03 | 2.62E+03 | | |
| TRIAL 2 | | | | | | | | | | | | | | |
| Reduction | Micro-CT | CBCT12 | CBCT18 | Micro-CT | CBCT12 | CBCT18 | Micro-CT | CBCT12 | CBCT18 | Micro-CT | CBCT12 | CBCT18 | | |
| 100% | 4.84E+02 | 5.18E+02 | 5.00E+02 | 2.43E+01 | 2.44E+01 | 2.42E+01 | 25983348 | 265367 | 18530 | 1.53E+02 | 3.00E+03 | 2.73E+03 | | |
| 50% | | 3.70E+02 | 3.55E+02 | | 2.44E+01 | 2.42E+01 | | 189438 | 13166 | | 3.13E+03 | 2.84E+03 | | |
| 25% | | 2.96E+02 | 2.84E+02 | | 2.44E+01 | 2.42E+01 | | 151533 | 10516 | | 3.25E+03 | 2.93E+03 | | |
| 12.50% | | 2.59E+02 | 2.47E+02 | | 2.44E+01 | 2.42E+01 | | 132554 | 9166 | | 3.33E+03 | 3.00E+03 | | |
| 6.25% | | 2.40E+02 | 2.30E+02 | | 2.44E+01 | 2.43E+01 | | 123039 | 8527 | | 3.38E+03 | 3.04E+03 | | |
| CEJ, Midroot, Apex | | 2.26E+02 | 2.21E+02 | | 1.86E+01 | 2.40E+01 | | 115671 | 8186 | | 3.43E+03 | 3.07E+03 | | |
| 3D Wrap Interpolation | | | | | | | | | | | | | | |
| 100% | 5.19E+02 | 6.01E+02 | 4.26E+02 | 2.43E+01 | 2.41E+01 | 2.26E+01 | 27875384 | 307542 | 15766 | 1.47E+02 | 2.54E+03 | 2.55E+03 | | |
| 50% | | 5.10E+02 | 3.93E+02 | | 2.42E+01 | 2.31E+01 | | 260873 | 14549 | | 2.98E+03 | 2.79E+03 | | |
| 25% | | 5.08E+02 | 3.89E+02 | | 2.42E+01 | 2.31E+01 | | 260276 | 14417 | | 2.98E+03 | 2.79E+03 | | |
| 12.50% | | 5.10E+02 | 3.89E+02 | | 2.41E+01 | 2.29E+01 | | 260918 | 14389 | | 2.98E+03 | 2.78E+03 | | |
| 6.25% | | 5.12E+02 | 3.87E+02 | | 2.41E+01 | 2.29E+01 | | 261888 | 14336 | | 2.96E+03 | 2.73E+03 | | |
| CEJ, Midroot, Apex | | 4.81E+02 | 3.55E+02 | | 2.40E+01 | 2.25E+01 | | 246243 | 13160 | | 2.85E+03 | 2.68E+03 | | |
| Interpolation Toolbox | | | | | | | | | | | | | | |
| 100% | | | | | | | | | | | | | | |
| 50% | | 5.18E+02 | 5.00E+02 | | 2.44E+01 | 2.42E+01 | | 265323 | 18516 | | 3.00E+03 | 2.73E+03 | | |
| 25% | | 5.18E+02 | 5.01E+02 | | 2.44E+01 | 2.42E+01 | | 265312 | 18545 | | 3.00E+03 | 2.72E+03 | | |
| 12.50% | | 5.18E+02 | 5.01E+02 | | 2.44E+01 | 2.42E+01 | | 265295 | 18552 | | 3.00E+03 | 2.72E+03 | | |
| 6.25% | | 5.17E+02 | 5.05E+02 | | 2.44E+01 | 2.42E+01 | | 264774 | 18711 | | 3.00E+03 | 2.67E+03 | | |
| CEJ, Midroot, Apex | | 4.78E+02 | 4.77E+02 | | 2.44E+01 | 2.42E+01 | | 244670 | 17675 | | 2.97E+03 | 2.65E+03 | | |
| TRIAL 3 | | | | | | | | | | | | | | |
| Reduction | Micro-CT | CBCT12 | CBCT18 | Micro-CT | CBCT12 | CBCT18 | Micro-CT | CBCT12 | CBCT18 | Micro-CT | CBCT12 | CBCT18 | | |
| 100% | 4.84E+02 | 5.11E+02 | 5.12E+02 | 2.43E+01 | 2.44E+01 | 2.42E+01 | 25983970 | 258487 | 18997 | 1.53E+02 | 3.05E+03 | 2.69E+03 | | |
| 50% | | 3.64E+02 | 3.63E+02 | | 2.44E+01 | 2.42E+01 | | 184880 | 13459 | | 3.18E+03 | 2.80E+03 | | |
| 25% | | 2.91E+02 | 2.90E+02 | | 2.44E+01 | 2.42E+01 | | 148152 | 10730 | | 3.29E+03 | 2.90E+03 | | |
| 12.50% | | 2.57E+02 | 2.52E+02 | | 2.44E+01 | 2.42E+01 | | 129785 | 9338 | | 3.37E+03 | 2.97E+03 | | |
| 6.25% | | 2.39E+02 | 2.34E+02 | | 2.44E+01 | 2.43E+01 | | 120550 | 8680 | | 3.42E+03 | 3.01E+03 | | |
| 3.125% | | 2.28E+02 | 2.25E+02 | | 2.41E+01 | 2.41E+01 | | 115853 | 8320 | | 3.45E+03 | 3.04E+03 | | |
| CEJ, Midroot, Apex | | 2.23E+02 | 2.25E+02 | | 1.82E+01 | 2.40E+01 | | 113433 | 8331 | | 3.47E+03 | 3.04E+03 | | |
| 3D Wrap Interpolation | | | | | | | | | | | | | | |
| 100% | 5.20E+02 | 5.90E+02 | 4.23E+02 | 2.43E+01 | 2.40E+01 | 2.25E+01 | 27962245 | 299485 | 15759 | 1.46E+02 | 2.59E+03 | 2.48E+03 | | |
| 50% | | 5.00E+02 | 3.94E+02 | | 2.41E+01 | 2.31E+01 | | 255851 | 14579 | | 3.01E+03 | 2.74E+03 | | |
| 25% | | 5.00E+02 | 3.89E+02 | | 2.41E+01 | 2.31E+01 | | 255830 | 14390 | | 3.00E+03 | 2.75E+03 | | |
| 12.50% | | 5.02E+02 | 3.86E+02 | | 2.41E+01 | 2.30E+01 | | 256814 | 14292 | | 3.00E+03 | 2.74E+03 | | |
| 6.25% | | 5.04E+02 | 3.82E+02 | | 2.41E+01 | 2.30E+01 | | 258005 | 14154 | | 2.98E+03 | 2.69E+03 | | |
| 3.125% | | 4.98E+02 | 3.47E+02 | | 2.41E+01 | 2.15E+01 | | 255071 | 12865 | | 2.95E+03 | 2.55E+03 | | |
| CEJ, Midroot, Apex | | 4.72E+02 | 3.58E+02 | | 2.39E+01 | 2.27E+01 | | 241588 | 13267 | | 2.87E+03 | 2.60E+03 | | |
| Interpolation Toolbox | | | | | | | | | | | | | | |
| 100% | | | | | | | | | | | | | | |
| 50% | | 5.11E+02 | 5.12E+02 | | 2.44E+01 | 2.42E+01 | | 258325 | 19018 | | 3.05E+03 | 2.69E+03 | | |
| 25% | | 5.10E+02 | 5.15E+02 | | 2.44E+01 | 2.42E+01 | | 258257 | 19071 | | 3.05E+03 | 2.68E+03 | | |
| 12.50% | | 5.10E+02 | 5.13E+02 | | 2.44E+01 | 2.42E+01 | | 258283 | 19011 | | 3.05E+03 | 2.68E+03 | | |
| 6.25% | | 5.09E+02 | 5.17E+02 | | 2.44E+01 | 2.42E+01 | | 257506 | 19143 | | 3.05E+03 | 2.64E+03 | | |
| 3.125% | | 4.95E+02 | 5.03E+02 | | 2.44E+01 | 2.42E+01 | | 253133 | 18617 | | 3.05E+03 | 2.61E+03 | | |
| CEJ, Midroot, Apex | | 4.66E+02 | 4.89E+02 | | 2.44E+01 | 2.42E+01 | | 238095 | 18108 | | 3.01E+03 | 2.62E+03 | | |

Mandibular Left First Premolar

| TRIAL 1 | | | | | | | | | | | | |
|------------------------------|----------|----------|----------|----------|----------|----------|-------------|--------|--------|------------------|----------|----------|
| Reduction | Volume | | | Length | | | Voxel Count | | | Grayscale Values | | |
| | Micro-CT | CBCT12 | CBCT18 | Micro-CT | CBCT12 | CBCT18 | Micro-CT | CBCT12 | CBCT18 | Micro-CT | CBCT12 | CBCT18 |
| 100% | 4.88E+02 | 4.78E+02 | 5.05E+02 | 2.46E+01 | 2.37E+01 | 2.38E+01 | 26245466 | 244983 | 18687 | 1.54E+02 | 2.39E+03 | 1.88E+03 |
| 50% | | 3.51E+02 | 3.71E+02 | | 2.37E+01 | 2.38E+01 | | 179539 | 13754 | | 2.41E+03 | 1.90E+03 |
| 25% | | 2.87E+02 | 3.05E+02 | | 2.37E+01 | 2.38E+01 | | 146850 | 11294 | | 2.44E+03 | 1.92E+03 |
| 12.50% | | 2.55E+02 | 2.71E+02 | | 2.37E+01 | 2.38E+01 | | 130469 | 10055 | | 2.45E+03 | 1.93E+03 |
| 6.25% | | 2.39E+02 | 2.55E+02 | | 2.37E+01 | 2.38E+01 | | 122275 | 9445 | | 2.46E+03 | 1.93E+03 |
| 3.125% | | 2.31E+02 | 2.47E+02 | | 2.37E+01 | 2.38E+01 | | 118109 | 9144 | | 2.46E+03 | 1.94E+03 |
| CEJ, Midroot, Apex | | 2.26E+02 | 2.47E+02 | | 2.37E+01 | 2.38E+01 | | 115863 | 9153 | | 2.47E+03 | 1.94E+03 |
| 3D Wrap Interpolation | | | | | | | | | | | | |
| 100% | 5.25E+02 | 4.93E+02 | 3.71E+02 | 2.39E+01 | 2.33E+01 | 2.14E+01 | 28211910 | 252466 | 13755 | 1.47E+02 | 2.29E+03 | 1.90E+03 |
| 50% | | 4.79E+02 | 4.07E+02 | | 2.35E+01 | 2.20E+01 | | 245207 | 15072 | | 2.34E+03 | 1.89E+03 |
| 25% | | 4.77E+02 | 4.03E+02 | | 2.35E+01 | 2.20E+01 | | 244470 | 14936 | | 2.35E+03 | 1.89E+03 |
| 12.50% | | 4.77E+02 | 4.08E+02 | | 2.34E+01 | 2.23E+01 | | 244236 | 15113 | | 2.34E+03 | 1.88E+03 |
| 6.25% | | 4.77E+02 | 4.02E+02 | | 2.35E+01 | 2.23E+01 | | 244118 | 14883 | | 2.34E+03 | 1.88E+03 |
| 3.125% | | 4.70E+02 | 3.26E+02 | | 2.34E+01 | 2.06E+01 | | 240848 | 12081 | | 2.35E+03 | 1.88E+03 |
| CEJ, Midroot, Apex | | 4.49E+02 | 3.45E+02 | | 2.35E+01 | 2.14E+01 | | 230109 | 12779 | | 2.36E+03 | 1.91E+03 |
| Interpolation Toolbox | | | | | | | | | | | | |
| 100% | | | | | | | | | | | | |
| 50% | | 4.79E+02 | 5.05E+02 | | 2.37E+01 | 2.38E+01 | | 245038 | 18697 | | 2.39E+03 | 1.88E+03 |
| 25% | | 4.79E+02 | 5.05E+02 | | 2.37E+01 | 2.38E+01 | | 245047 | 18689 | | 2.39E+03 | 1.88E+03 |
| 12.50% | | 4.78E+02 | 5.05E+02 | | 2.37E+01 | 2.38E+01 | | 244838 | 18704 | | 2.39E+03 | 1.88E+03 |
| 6.25% | | 4.78E+02 | 5.03E+02 | | 2.37E+01 | 2.38E+01 | | 244589 | 18632 | | 2.38E+03 | 1.88E+03 |
| 3.125% | | 4.71E+02 | 4.91E+02 | | 2.37E+01 | 2.38E+01 | | 241402 | 18169 | | 2.39E+03 | 1.88E+03 |
| CEJ, Midroot, Apex | | 4.49E+02 | 4.78E+02 | | 2.37E+01 | 2.38E+01 | | 229927 | 17694 | | 2.41E+03 | 1.90E+03 |

| TRIAL 2 | | | | | | | | | | | | |
|------------------------------|----------|----------|----------|----------|----------|----------|-------------|--------|--------|------------------|----------|----------|
| Reduction | Volume | | | Length | | | Voxel Count | | | Grayscale Values | | |
| | Micro-CT | CBCT12 | CBCT18 | Micro-CT | CBCT12 | CBCT18 | Micro-CT | CBCT12 | CBCT18 | Micro-CT | CBCT12 | CBCT18 |
| 100% | 4.88E+02 | 4.99E+02 | 4.59E+02 | 2.46E+01 | 2.38E+01 | 2.33E+01 | 26245466 | 255710 | 17001 | 1.54E+02 | 2.35E+03 | 1.95E+03 |
| 50% | | 3.63E+02 | 3.40E+02 | | 2.38E+01 | 2.33E+01 | | 186059 | 12586 | | 2.38E+03 | 1.97E+03 |
| 25% | | 2.95E+02 | 2.80E+02 | | 2.38E+01 | 2.33E+01 | | 151187 | 10380 | | 2.40E+03 | 1.98E+03 |
| 12.50% | | 2.61E+02 | 2.51E+02 | | 2.38E+01 | 2.33E+01 | | 133833 | 9303 | | 2.42E+03 | 1.99E+03 |
| 6.25% | | 2.44E+02 | 2.36E+02 | | 2.38E+01 | 2.33E+01 | | 125168 | 8737 | | 2.43E+03 | 2.00E+03 |
| CEJ, Midroot, Apex | | 2.31E+02 | 2.29E+02 | | 2.36E+01 | 2.33E+01 | | 118302 | 8489 | | 2.44E+03 | 2.00E+03 |
| 3D Wrap Interpolation | | | | | | | | | | | | |
| 100% | 5.25E+02 | 5.09E+02 | 3.49E+02 | 2.40E+01 | 2.34E+01 | 2.15E+01 | 28211918 | 260699 | 12917 | 1.47E+02 | 2.28E+03 | 1.90E+03 |
| 50% | | 3.63E+02 | 3.67E+02 | | 2.38E+01 | 2.23E+01 | | 186059 | 13606 | | 2.38E+03 | 1.90E+03 |
| 25% | | 4.99E+02 | 3.67E+02 | | 2.36E+01 | 2.20E+01 | | 255527 | 13583 | | 2.32E+03 | 1.90E+03 |
| 12.50% | | 5.04E+02 | 3.71E+02 | | 2.36E+01 | 2.20E+01 | | 257974 | 13741 | | 2.30E+03 | 1.89E+03 |
| 6.25% | | 5.12E+02 | 3.55E+02 | | 2.36E+01 | 2.20E+01 | | 262129 | 13144 | | 2.27E+03 | 1.90E+03 |
| CEJ, Midroot, Apex | | 4.80E+02 | 3.33E+02 | | 2.30E+01 | 2.17E+01 | | 245648 | 12324 | | 2.24E+03 | 1.90E+03 |
| Interpolation Toolbox | | | | | | | | | | | | |
| 100% | | | | | | | | | | | | |
| 50% | | 4.99E+02 | 4.58E+02 | | 2.38E+01 | 2.33E+01 | | 255703 | 16976 | | 2.35E+03 | 1.95E+03 |
| 25% | | 4.99E+02 | 4.58E+02 | | 2.38E+01 | 2.33E+01 | | 255594 | 16970 | | 2.35E+03 | 1.95E+03 |
| 12.50% | | 4.99E+02 | 4.60E+02 | | 2.38E+01 | 2.33E+01 | | 255612 | 17030 | | 2.35E+03 | 1.95E+03 |
| 6.25% | | 5.00E+02 | 4.50E+02 | | 2.38E+01 | 2.33E+01 | | 256022 | 16654 | | 2.34E+03 | 1.95E+03 |
| CEJ, Midroot, Apex | | 4.61E+02 | 4.40E+02 | | 2.38E+01 | 2.33E+01 | | 236193 | 16286 | | 2.37E+03 | 1.95E+03 |

| TRIAL 3 | | | | | | | | | | | | |
|------------------------------|----------|----------|----------|----------|----------|----------|-------------|--------|--------|------------------|----------|----------|
| Reduction | Volume | | | Length | | | Voxel Count | | | Grayscale Values | | |
| | Micro-CT | CBCT12 | CBCT18 | Micro-CT | CBCT12 | CBCT18 | Micro-CT | CBCT12 | CBCT18 | Micro-CT | CBCT12 | CBCT18 |
| 100% | 4.88E+02 | 4.99E+02 | 4.66E+02 | 2.46E+01 | 2.38E+01 | 2.33E+01 | 26245466 | 255710 | 17270 | 1.54E+02 | 2.35E+03 | 1.94E+03 |
| 50% | | 3.63E+02 | 3.45E+02 | | 2.38E+01 | 2.33E+01 | | 186059 | 12776 | | 2.38E+03 | 1.96E+03 |
| 25% | | 2.95E+02 | 2.84E+02 | | 2.38E+01 | 2.33E+01 | | 151187 | 10527 | | 2.40E+03 | 1.97E+03 |
| 12.50% | | 2.61E+02 | 2.54E+02 | | 2.38E+01 | 2.33E+01 | | 133833 | 9426 | | 2.42E+03 | 1.98E+03 |
| 6.25% | | 2.44E+02 | 2.39E+02 | | 2.38E+01 | 2.33E+01 | | 125168 | 8850 | | 2.43E+03 | 1.99E+03 |
| CEJ, Midroot, Apex | | 2.31E+02 | 2.32E+02 | | 2.36E+01 | 2.33E+01 | | 118302 | 8597 | | 2.44E+03 | 1.99E+03 |
| 3D Wrap Interpolation | | | | | | | | | | | | |
| 100% | 5.25E+02 | 5.09E+02 | 3.59E+02 | 2.39E+01 | 2.34E+01 | 2.11E+01 | 28211910 | 260699 | 13281 | 1.47E+02 | 2.28E+03 | 1.91E+03 |
| 50% | | 4.99E+02 | 3.75E+02 | | 2.36E+01 | 2.21E+01 | | 255579 | 13902 | | 2.32E+03 | 1.91E+03 |
| 25% | | 4.99E+02 | 3.78E+02 | | 2.36E+01 | 2.20E+01 | | 255527 | 14012 | | 2.32E+03 | 1.91E+03 |
| 12.50% | | 5.04E+02 | 3.81E+02 | | 2.36E+01 | 2.21E+01 | | 257974 | 14093 | | 2.30E+03 | 1.90E+03 |
| 6.25% | | 5.12E+02 | 3.67E+02 | | 2.36E+01 | 2.20E+01 | | 262129 | 13588 | | 2.27E+03 | 1.90E+03 |
| CEJ, Midroot, Apex | | 4.80E+02 | 3.43E+02 | | 2.33E+01 | 2.17E+01 | | 245648 | 12714 | | 2.24E+03 | 1.90E+03 |
| Interpolation Toolbox | | | | | | | | | | | | |
| 100% | | | | | | | | | | | | |
| 50% | | 4.99E+02 | 4.66E+02 | | 2.38E+01 | 2.33E+01 | | 255703 | 17244 | | 2.35E+03 | 1.94E+03 |
| 25% | | 4.99E+02 | 4.65E+02 | | 2.38E+01 | 2.33E+01 | | 255594 | 17237 | | 2.35E+03 | 1.94E+03 |
| 12.50% | | 4.99E+02 | 4.67E+02 | | 2.38E+01 | 2.33E+01 | | 255612 | 17286 | | 2.35E+03 | 1.94E+03 |
| 6.25% | | 5.00E+02 | 4.57E+02 | | 2.38E+01 | 2.33E+01 | | 256022 | 16915 | | 2.34E+03 | 1.95E+03 |
| CEJ, Midroot, Apex | | 4.61E+02 | 4.47E+02 | | 2.38E+01 | 2.33E+01 | | 236193 | 16549 | | 2.37E+03 | 1.95E+03 |

Mandibular Right Central Incisor

| TRIAL 1 | | | | | | | | | | | | |
|------------------------------|----------|----------|----------|----------|----------|----------|-------------|--------|--------|------------------|----------|----------|
| Reduction | Volume | | | Length | | | Voxel Count | | | Grayscale Values | | |
| | Micro-CT | CBCT12 | CBCT18 | Micro-CT | CBCT12 | CBCT18 | Micro-CT | CBCT12 | CBCT18 | Micro-CT | CBCT12 | CBCT18 |
| 100% | 2.33E+02 | 2.22E+02 | 2.51E+02 | 2.11E+01 | 2.09E+01 | 2.11E+01 | 12501464 | 113438 | 9304 | 1.64E+02 | 2.36E+03 | 1.87E+03 |
| 50% | | 1.62E+02 | 1.89E+02 | | 2.10E+01 | 2.11E+01 | | 83037 | 6986 | | 2.36E+03 | 1.88E+03 |
| 25% | | 1.32E+02 | 1.57E+02 | | 2.10E+01 | 2.11E+01 | | 67810 | 5829 | | 2.37E+03 | 1.88E+03 |
| 12.50% | | 1.18E+02 | 1.42E+02 | | 2.09E+01 | 2.11E+01 | | 60231 | 5248 | | 2.37E+03 | 1.89E+03 |
| 6.25% | | 1.10E+02 | 1.34E+02 | | 2.09E+01 | 2.11E+01 | | 56449 | 4967 | | 2.37E+03 | 1.89E+03 |
| CEJ, Midroot, Apex | | 1.05E+02 | 1.32E+02 | | 2.09E+01 | 2.11E+01 | | 53763 | 4894 | | 2.37E+03 | 1.89E+03 |
| 3D Wrap Interpolation | | | | | | | | | | | | |
| 100% | 2.31E+02 | 2.18E+02 | 1.56E+02 | 1.95E+01 | 2.04E+01 | 1.84E+01 | 12421668 | 111486 | 5793 | 1.60E+02 | 2.27E+03 | 1.97E+03 |
| 50% | | 2.13E+02 | 1.78E+02 | | 2.09E+01 | 1.94E+01 | | 109281 | 6590 | | 2.33E+03 | 1.96E+03 |
| 25% | | 2.11E+02 | 1.75E+02 | | 2.03E+01 | 1.91E+01 | | 108234 | 6488 | | 2.34E+03 | 1.96E+03 |
| 12.50% | | 2.12E+02 | 1.71E+02 | | 2.05E+01 | 1.91E+01 | | 108639 | 6327 | | 2.33E+03 | 1.95E+03 |
| 6.25% | | 2.13E+02 | 1.62E+02 | | 2.05E+01 | 1.91E+01 | | 108915 | 6013 | | 2.32E+03 | 1.92E+03 |
| CEJ, Midroot, Apex | | 1.95E+02 | 1.50E+02 | | 2.04E+01 | 1.84E+01 | | 100004 | 5570 | | 2.30E+03 | 1.89E+03 |
| Interpolation Toolbox | | | | | | | | | | | | |
| 100% | | | | | | | | | | | | |
| 50% | | 2.22E+02 | 2.51E+02 | | 2.09E+01 | 2.11E+01 | | 113556 | 9299 | | 2.36E+03 | 1.87E+03 |
| 25% | | 2.22E+02 | 2.51E+02 | | 2.09E+01 | 2.11E+01 | | 113547 | 9292 | | 2.36E+03 | 1.87E+03 |
| 12.50% | | 2.22E+02 | 2.51E+02 | | 2.09E+01 | 2.11E+01 | | 113537 | 9299 | | 2.35E+03 | 1.87E+03 |
| 6.25% | | 2.21E+02 | 2.49E+02 | | 2.09E+01 | 2.11E+01 | | 113315 | 9223 | | 2.35E+03 | 1.87E+03 |
| CEJ, Midroot, Apex | | 2.06E+02 | 2.45E+02 | | 2.10E+01 | 2.11E+01 | | 105288 | 9070 | | 2.36E+03 | 1.87E+03 |

| TRIAL 2 | | | | | | | | | | | | |
|------------------------------|----------|----------|----------|----------|----------|----------|-------------|--------|--------|------------------|----------|----------|
| Reduction | Volume | | | Length | | | Voxel Count | | | Grayscale Values | | |
| | Micro-CT | CBCT12 | CBCT18 | Micro-CT | CBCT12 | CBCT18 | Micro-CT | CBCT12 | CBCT18 | Micro-CT | CBCT12 | CBCT18 |
| 100% | 2.33E+02 | 2.23E+02 | 2.16E+02 | 2.11E+01 | 2.09E+01 | 2.04E+01 | 12501464 | 11346 | 8017 | 1.64E+02 | 2.36E+03 | 2.00E+03 |
| 50% | | 1.62E+02 | 1.64E+02 | | 2.10E+01 | 2.04E+01 | | 83037 | 6086 | | 2.36E+03 | 2.00E+03 |
| 25% | | 1.31E+02 | 1.38E+02 | | 2.10E+01 | 2.04E+01 | | 67808 | 5123 | | 2.37E+03 | 2.00E+03 |
| 12.50% | | 1.18E+02 | 1.25E+02 | | 2.09E+01 | 2.04E+01 | | 60231 | 4640 | | 2.37E+03 | 1.99E+03 |
| 6.25% | | 1.10E+02 | 1.19E+02 | | 2.09E+01 | 2.04E+01 | | 56449 | 4402 | | 2.37E+03 | 1.99E+03 |
| CEJ, Midroot, Apex | | 1.05E+02 | 1.17E+02 | | 2.09E+01 | 2.04E+01 | | 53763 | 4339 | | 2.37E+03 | 2.00E+03 |
| 3D Wrap Interpolation | | | | | | | | | | | | |
| 100% | 2.31E+02 | 2.17E+02 | 1.17E+02 | 1.95E+01 | 2.03E+01 | 1.78E+01 | 12421668 | 111486 | 4347 | 1.60E+02 | 2.27E+03 | 1.98E+03 |
| 50% | | 2.13E+02 | 1.36E+02 | | 2.05E+01 | 1.87E+01 | | 109281 | 5019 | | 2.33E+03 | 2.00E+03 |
| 25% | | 2.11E+02 | 1.33E+02 | | 2.05E+01 | 1.84E+01 | | 108234 | 4934 | | 2.34E+03 | 2.00E+03 |
| 12.50% | | 2.12E+02 | 1.34E+02 | | 2.05E+01 | 1.84E+01 | | 108639 | 4957 | | 2.33E+03 | 1.99E+03 |
| 6.25% | | 2.13E+02 | 1.23E+02 | | 2.05E+01 | 1.84E+01 | | 108915 | 4563 | | 2.32E+03 | 1.95E+03 |
| CEJ, Midroot, Apex | | 1.95E+02 | 1.10E+02 | | 2.04E+01 | 1.70E+01 | | 100004 | 4085 | | 2.30E+03 | 1.92E+03 |
| Interpolation Toolbox | | | | | | | | | | | | |
| 100% | | | | | | | | | | | | |
| 50% | | 2.22E+02 | 2.16E+02 | | 2.09E+01 | 2.04E+01 | | 113556 | 7989 | | 2.36E+03 | 2.00E+03 |
| 25% | | 2.22E+02 | 2.15E+02 | | 2.09E+01 | 2.04E+01 | | 113547 | 7972 | | 2.36E+03 | 2.00E+03 |
| 12.50% | | 2.22E+02 | 2.16E+02 | | 2.09E+01 | 2.04E+01 | | 113537 | 7983 | | 2.35E+03 | 2.00E+03 |
| 6.25% | | 2.21E+02 | 2.11E+02 | | 2.09E+01 | 2.04E+01 | | 113315 | 7824 | | 2.35E+03 | 2.00E+03 |
| CEJ, Midroot, Apex | | 2.06E+02 | 2.05E+02 | | 2.10E+01 | 2.04E+01 | | 105288 | 7601 | | 2.36E+03 | 2.00E+03 |

| TRIAL 3 | | | | | | | | | | | | |
|------------------------------|----------|----------|----------|----------|----------|----------|-------------|--------|--------|------------------|----------|----------|
| Reduction | Volume | | | Length | | | Voxel Count | | | Grayscale Values | | |
| | Micro-CT | CBCT12 | CBCT18 | Micro-CT | CBCT12 | CBCT18 | Micro-CT | CBCT12 | CBCT18 | Micro-CT | CBCT12 | CBCT18 |
| 100% | 2.33E+02 | 2.03E+02 | 2.14E+02 | 2.11E+01 | 2.09E+01 | 2.04E+01 | 12501464 | 103833 | 8015 | 1.64E+02 | 2.42E+03 | 2.00E+03 |
| 50% | | 1.48E+02 | 1.62E+02 | | 2.09E+01 | 2.04E+01 | | 75799 | 6085 | | 2.43E+03 | 2.00E+03 |
| 25% | | 1.21E+02 | 1.37E+02 | | 2.09E+01 | 2.04E+01 | | 61774 | 5123 | | 2.44E+03 | 2.00E+03 |
| 12.50% | | 1.07E+02 | 1.23E+02 | | 2.09E+01 | 2.04E+01 | | 54784 | 4640 | | 2.44E+03 | 1.99E+03 |
| 6.25% | | 1.00E+02 | 1.19E+02 | | 2.09E+01 | 2.04E+01 | | 51329 | 4402 | | 2.44E+03 | 1.99E+03 |
| CEJ, Midroot, Apex | | 9.54E+01 | 1.17E+02 | | 2.08E+01 | 2.04E+01 | | 48868 | 4339 | | 2.44E+03 | 2.00E+03 |
| 3D Wrap Interpolation | | | | | | | | | | | | |
| 100% | 2.31E+02 | 2.04E+02 | 1.16E+02 | 1.95E+01 | 2.00E+01 | 1.78E+01 | 12421668 | 104648 | 4347 | 1.60E+02 | 2.30E+03 | 1.98E+03 |
| 50% | | 1.99E+02 | 1.34E+02 | | 2.04E+01 | 1.87E+01 | | 102120 | 5019 | | 2.37E+03 | 2.00E+03 |
| 25% | | 1.98E+02 | 1.33E+02 | | 2.04E+01 | 1.84E+01 | | 101524 | 4934 | | 2.37E+03 | 2.00E+03 |
| 12.50% | | 1.98E+02 | 1.33E+02 | | 2.04E+01 | 1.84E+01 | | 101327 | 4957 | | 2.36E+03 | 1.99E+03 |
| 6.25% | | 1.99E+02 | 1.21E+02 | | 2.04E+01 | 1.84E+01 | | 101986 | 4563 | | 2.36E+03 | 1.95E+03 |
| CEJ, Midroot, Apex | | 1.74E+02 | 1.10E+02 | | 2.01E+01 | 1.70E+01 | | 89175 | 4085 | | 2.37E+03 | 1.92E+03 |
| Interpolation Toolbox | | | | | | | | | | | | |
| 100% | | | | | | | | | | | | |
| 50% | | 2.03E+02 | 2.14E+02 | | 2.09E+01 | 2.04E+01 | | 104067 | 7989 | | 2.42E+03 | 2.00E+03 |
| 25% | | 2.03E+02 | 2.15E+02 | | 2.09E+01 | 2.04E+01 | | 103829 | 7972 | | 2.42E+03 | 2.00E+03 |
| 12.50% | | 2.02E+02 | 2.14E+02 | | 2.09E+01 | 2.04E+01 | | 103664 | 7983 | | 2.42E+03 | 2.00E+03 |
| 6.25% | | 2.02E+02 | 2.10E+02 | | 2.09E+01 | 2.04E+01 | | 103452 | 7824 | | 2.41E+03 | 2.00E+03 |
| CEJ, Midroot, Apex | | 1.89E+02 | 2.05E+02 | | 2.09E+01 | 2.04E+01 | | 96829 | 7601 | | 2.41E+03 | 2.00E+03 |